THE ROLE OF STEREOREGULARITY IN CONTROLLING

THE SOLIDIFICATION OF POLYPROPYLENE FROM THE MELT

by

Michael E A Cudby

A thesis in support of candidature

for the degree of Master of Philosophy

at the

University of Southampton

July 1982

# Acknowledgements

ABSTRACT

FACULTY OF SCIENCE

CHEMISTRY

## Master of Philosophy

THE ROLE OF STEREOREGULARITY IN CONTROLLING THE SOLIDIFICATION
OF POLYPROPYLENE FROM THE MELT
by Michael E A CUDBY

A study has been made of the influence of the degree
of stereoregularity on the crystallisation and solidification
processes in essentially isotactic polypropylene.  Three
gas phase polymerised materials have been examined both in the
'as made' condition and after hydrocarbon extraction to remove
soluble low molecular weight and atactic polymer.  The whole
polymers and the hydrocarbon insoluble fractions were subjected
to molecular weight determination, differential scanning
calorimetry, infrared, x-ray and NMR spectroscopy.  It was
found that the extraction process reduced the irregular
sequences known as racemic dyads with a consequent increase in
the rate of helix formation determined by infrared techniques.
The ultimate crystallinity is seen to decrease with increasing
molecular weight and it appears that the racemic dyad
concentration and ultimate crystallinity are inversely related.
Increasing the racemic dyad concentration leads to a decrease
in the physical property known as the flexural modulus and a
linear relationship between these values is observed.

# CONTENTS

CHAPTER 1

INTRODUCTION

Large scale production of polypropylene began in the late 1950's making the third largest scale production polymer after polyethylene and polyvinylchloride. The commercial interest in polypropylene is due to its very different physical properties compared with the polyethylene then produced (using a high pressure process and having a density of the order 0.92 g/cm$^3$. The melting point of polypropylene approaches 170$^{\circ}$C whereas polyethylene has a melting point at the quoted density of approaching 110$^{\circ}$C, clearly an advantage in many areas where rigidity at elevated temperatures is required.. Other physical properties of polypropylene which differ concern toughness, surface quality, clarity as film etc.

The introduction of the Ziegler-Natta catalyst for olefin polymerisation in 1952 revolutionised the polymer industry and allowed the preparation of a highly stereoregular product in many cases including polypropylene. Natta (1) observed that the product of this type of polymerisation could be separated into crystalline and amorphous components by their solubility in organic solvents. The crystalline form was obtained as the insoluble fraction of a heptane extraction whereas the amorphous component was obtained in a pure state as the ether extract. Any monomer which contains an asymmetric carbon atom can in principle give rise to a number of stereo isomeric forms. X-ray analysis by Natta of the crystalline product of this new polymerisation process led to the belief that all the asymmetric carbon atoms in the molecule contained within the crystal lattice must have the same steric configuration. Further, Natta proposed that in the case of polypropylene all the methyl groups must be placed on the same side of the plane of a fully extended molecular chain. The term 'isotactic' was also given by Natta (2) to this configuration and this has been universally adopted. The presence of steric irregularities in the essentially isotactic chain was considered at a later date. Such irregularities were recognised by their effect in lowering the melting point of the crystalline polymer. These

irregularities are therefore to be thought of as mistakes in the polymerisation process and can be defined structurally as described by Bovey (3) and discussed later, and it is these imperfections and their effect on physical properties which forms the subject of this study.
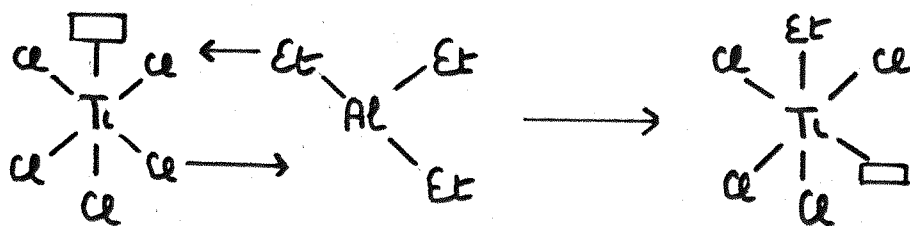
## Catalysis

The catalyst used is based on the discovery by Ziegler in 1953 of a heterogeneous system comprising titanium trichloride plus an aluminium alkyl in an inert aliphatic diluent. Titanium trichloride ($TiCl_3$) can exist in a number of crystalline forms known as $\alpha$, $\beta$, $\gamma$ and $\delta$ (4,5). The most stereo-regulating form is the $\alpha$-crystalline form which exists as a violet compound having a layer structure of $Ti^{3+}$ and $Cl^-$ atoms (6) with the $Ti^{3+}$ residing in a site of coordination number six. In the $\alpha$-form the titanium layers lie interstitially between chlorine layers with the chlorine atoms in a close packed hexagonal array. Although $\alpha$-$TiCl_3$ alone will polymerise propylene, the presence of the activator based on aluminium alkyls or alkyl chlorides greatly increases the rate of polymerisation and yet still produces a highly stereoregular polymer.

The mechanism by which the catalyst produces polypropylene is still less than fully understood and many theories have been put forward. A number of reviews have appeared which indicate the complexity of this catalyst system and also show the current views on the mechanism of polymerisation and stereo-regulation. The active centres for polymer growth are currently considered to be associated with the edges or lateral planes of the $\alpha$-$TiCl_3$ crystal (7,8). In a recent review (9) Caunt comments that high activity is gained by dry milling to achieve a reduction in crystallite size. Further, the first few seconds of polymerisation results in the break up of agglomerated crystals and this is seen as an essential part in the production of a high concentration of active centres.

A mechanism for the production of active centres involving the interaction of $TiCl_3$ with an aluminium alkyl was proposed (10,11) and this is still considered to be essentially correct. The following scheme is proposed which

involves a chlorine vacancy produced in the TiCl$_3$ lattice during the preparation.



The polymerisation process then follows the route
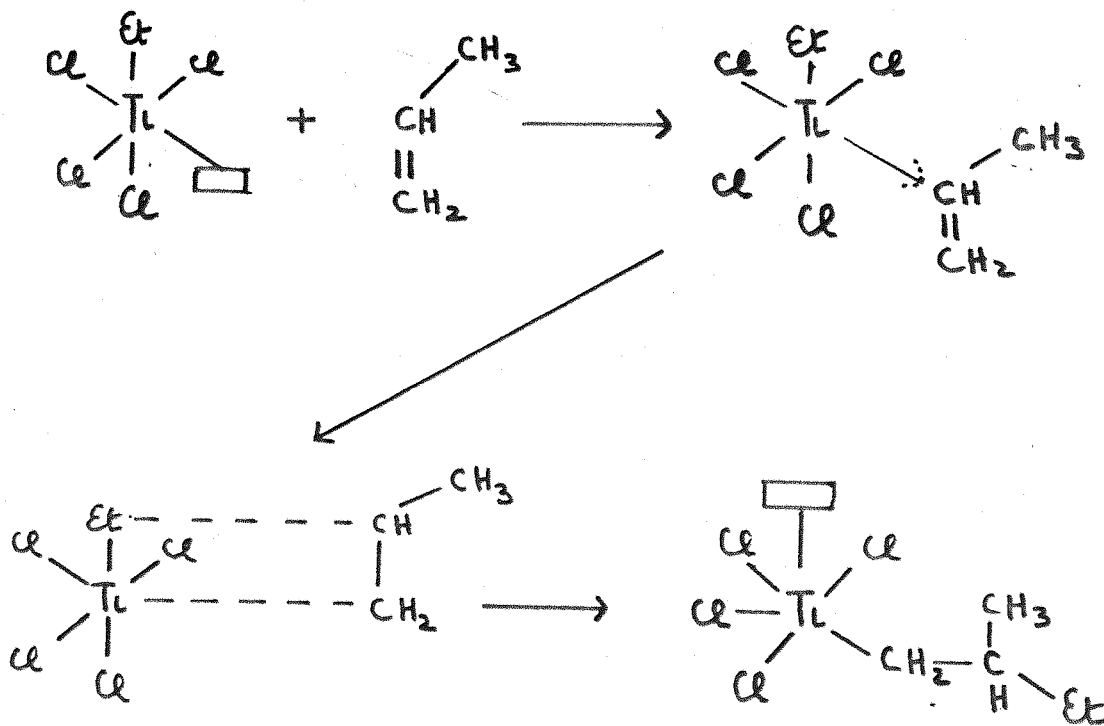


However, the production of the isotactic stereoregular polymer is not well understood. Zambelli (12) states that the nearly stoichiometric reaction between monomer and catalyst supports the view that isotactic polymerisation proceeds via a monomer insertion mechanism and further, polymerisation of 1 - d$_1$ - deuteropropene has established that the double bond opens in the cis direction (13, 14, 15). According to the Arlman-Corsee theory (16) the production of isotactic polymer

is due to steric hindrance arising from the interaction of a monomer unit with the asymmetric catalyst active centre and in particular with the chlorine atoms bonded to the titanium atom in the complex.

The gas phase polymerisation of propene is a recent innovation with a number of patents describing processes aimed at high conversion to polymer of a highly isotactic nature. A number of processes involve grinding titanium trichloride with a variety of Lewis bases but the details of the stereoregulating polymerisation process are not divulged. One such process has been used to produce the polymers used for this study.

## Stereoisomerism in polypropylene and the proton NMR spectrum

When a polymerising monomer possesses an asymmetric centre then it is possible that different stereoisomeric forms will exist in the polymer molecule. This has been mentioned in the introduction but a more detailed examination of these stereoisomers is more appropriate in this section. In terms of a planar presentation of an extended molecule the following structures are apparent.



ISOTACTIC

SYNDIOTACTIC

HETEROTACTIC
(ATACTIC)
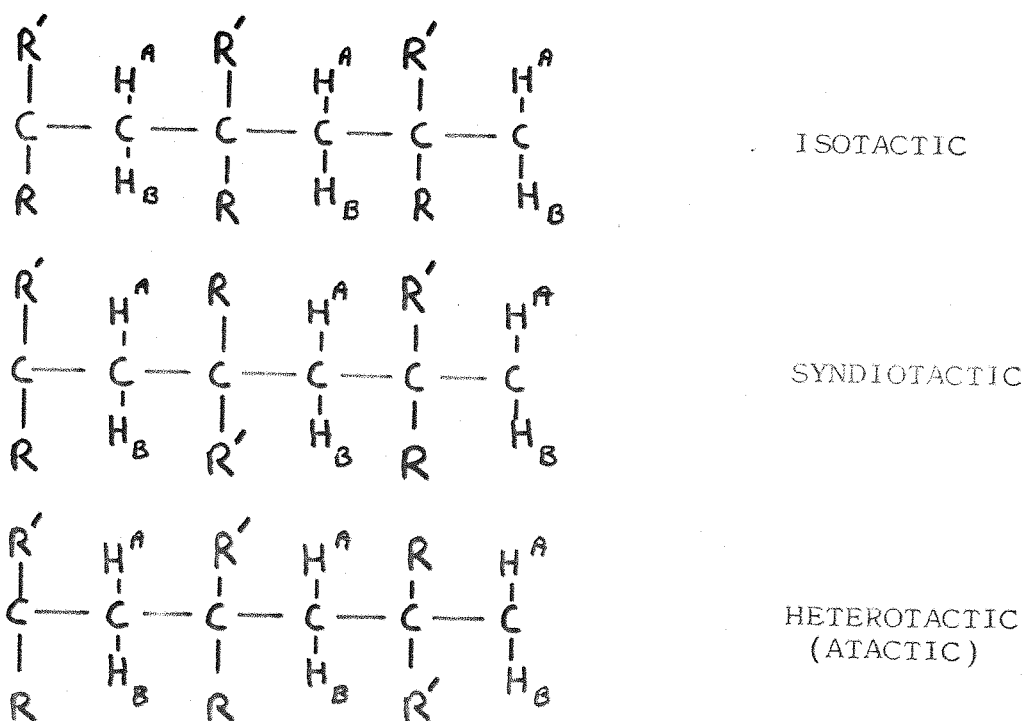
The geometric equivalence or otherwise of the protons in the methylene group $H^A$ and $H_B$, is of importance in the proton NMR spectrum. In the isotactic form the protons labelled $H^A$ are in a similar environment and different to those labelled $H_B$. In the syndiotactic form the environments of $H^A$ and $H_B$ are for the purposes of this discussion to be considered equivalent. The heterotactic form (atactic) will obviously contain structures which are admixtures of both isotactic and syndiotactic forms. In NMR studies it is generally understood that geometrically non-equivalent nuclei will exhibit magnetic non-equivalence. This in turn will result in these nuclei having different chemical shifts and different coupling will be evident between the nuclei. It should therefore be possible to distinguish the tacticity of the various polymeric stereoisomers by recourse to the coupling patterns and chemical shifts displayed. For example, in the isotactic case the non-equivalence of the methylene protons would be expected to result in a quartet of resonances. However, the syndiotactic species would be expected to give rise to a single resonance due to the apparent equivalence of the protons in the methylene group. This approach is real enough but it must be noted that a much more complicated resonance pattern will arise when $R'$ or R is a proton or some other magnetic species which can couple with the protons of the methylene group. In polypropylene the R group represents a proton and the $R'$ group the methyl group. Thus, significant coupling will take place between the protons of the methylene group and that of the methine and since the chemical shift difference between the interacting species is small, a complex coupling will result which is termed second order. The use of high field strength instrumentation improves the dispersion of the spectrum revealing peaks which at lower field strengths would overlap. At the same time the use of higher field strengths improves the signal to noise ratio. In the work to be described here a Perkin-Elmer R34, 220 MHz proton resonance spectrometer is used providing sufficient definition to satisfy the requirements of this structural examination.

Commercially available polypropylene contains very long molecular repeat units of the isotactic species. The physical properties associated with this polymer are the result of the

combination of molecules in crystalline and amorphous regions and their interactions. For example, the stiffness is associated with the degree of crystallinity whilst the toughness is controlled by the amorphous regions. The average value for the crystalline content of isotactic polypropylene in finished articles is between 60 and 70%, the result of the alignment of the isotactic molecules in three dimensional order. As the total modulus of heterogeneous polymers is a function of both crystalline and amorphous regions, the dependance of flexural modulus on racemic dyad content requires explanation. The perfection of crystalline regions depends upon the presence of long runs of isotactic molecules in the helical conformation to provide the stiff backbone of the heterogeneous mass. It can be demonstrated that the helical content of the total polymer is considerably higher than the crystalline content demands ( $>90\%$ ) thus, if the modulus is indeed more dependent upon the non-crystalline zones then the strength of molecules in these regions must also depend upon the presence of racemic units which locally disrupt the helical conformation. It is necessary to quantify these 'mistakes' in the molecular structure in order to comment on their significance in the solidification and crystallisation process. Further definition of the polymer molecular structure is required to identify these inconsistences. Bovey (3) has developed the use of dyad configurations wherein like dyads are described as meso (m) and unlike dyads as racemic (r). The stick diagram below is an example of the shorthand notation of m and r dyads which can be used to describe the steric configuration of a polypropylene molecule in terms of triads, tetrads etc.



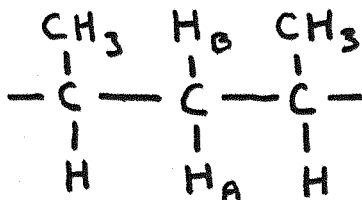Where $\bigsqcup$ is $-CH-CH_2-$ with $CH_3$ on the $CH$
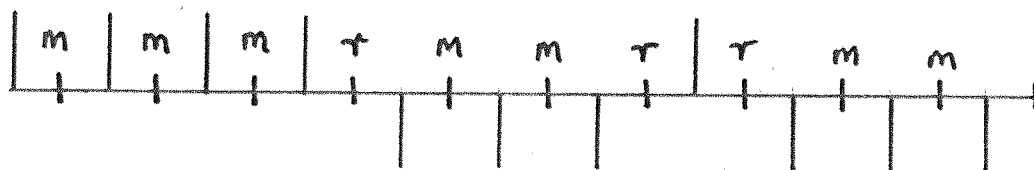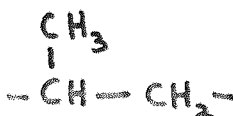
In order to make use of this definition it is necessary
to assign the NMR spectrum in terms of these dyad structures.
If a quantitative estimate is required then, if possible, a
proton magnetic resonance spectrum is more suitable and the
use of a continuous wave spectrometer will overcome the
difficulties of pulse repetition, different relaxation rates
and Nuclear Overhauser effects seen with Fourier transform
techniques.

## The assignment of the proton resonances in the NMR spectrum of polypropylene

The proton spectrum of polypropylene is one of considerable
complexity. The chemical shift differences between the
interacting methylene, methine and methyl groups are small and
therefore the coupling observed between the protons is as
designated second order. The high field strength of the magnet
system used to observe these resonances helps to reduce the
complexity of the spectrum by increasing the chemical shift
difference between the interacting protons. The assignment of
the observed resonances was begun as early as the 1960's  and
this work has been brought together in a publication by
Woodbrey (17). However. the advent of high field instrumentation
made the task more simple and a number of workers illustrated
the now nearly first order spectrum which would be obtained
from the essentially isotactic form of the polymer (18, 19).
The greater detail of resonances due to the different triad
and tetrad sequences described earlier have necessitated a
detailed study making use of models based on 'atactic' polymer
(20) deuterated systems (21) etc.

It is now possible to assign the 220 MHz proton spectrum
in terms of dyad and tetrad sequences as illustrated in figure 1.
These assignments are related to the structure of polypropylene
as shown previously. The molecular repeat unit of the polymer
is as follows:-

$$-\overset{\displaystyle CH_3}{\underset{\displaystyle H}{\overset{|}{\underset{|}{C}}}} - \overset{\displaystyle H_B}{\underset{\displaystyle H_A}{\overset{|}{\underset{|}{C}}}} - \overset{\displaystyle CH_3}{\underset{\displaystyle H}{\overset{|}{\underset{|}{C}}}} -$$

As described, the chemical shift of the methylene protons $H_B$ (the syn proton) and $H_A$ (the anti proton), are sufficiently different to give rise to significantly different chemical shifts and coupling patterns. The small amounts of non isotactic sequences present in the commercial polypropylenes used in this study are observed between the resonance assigned to the anti proton of the methylene group and the resonance assigned to the methyl protons. The assignment given indicates that this resonance is due to a combination of mrm, mrr and rrr tetrads although the latter is likely to be less significant due to the method of polymerisation. Different stereoregular structures are observed in the spectrum as a result of long range nonequivalence effects. If adjacent monomer units are concerned then the term dyad is used. For longer range effects, triad, tetrad and pentad terms are used. The recognition of dyads and tetrads requires the observation of the atoms of the $\beta$ group in the polymerised olefin whereas triads and pentads are recognised from resonances due to the $\alpha$ group.

## The $^{13}C$ spectrum of polypropylene

As with the proton, $^1H$, the $^{13}C$ isotope of carbon possesses the magnetic properties necessary to allow observation of the nuclear magnetic resonance spectrum i.e. nuclear spin or angular momentum and the associated magnetic moment. However, due to its natural abundance (1.1%) and sensitivity of 0.016 relative to the proton sensitivity given as 1.00, the observation of the spectrum requires the use of a pulse fourier transform technique. In this technique a high power radio frequency pulse is passed into the sample simultaneously exciting all the resonances of interest. At the end of the pulse period all the nuclei precess about the direction of the applied magnetic field with their characteristic frequencies. The resulting magnetisation induces a signal with an exponentially decaying amplitude. This signal is also called the free induction decay and contains the same information as the conventional spectrum obtained by a continuous sweep of the frequencies, the technique used to obtain the proton spectrum

described earlier. Many free induction decays are superimposed and stored in a computer memory and the accumulated data fourier tranformed to give the more easily recognised resonance spectrum. The $^{13}$C spectrum of the methyl carbon resonance of polypropylene is illustrated in figure 2. The inherently larger chemical shift difference in the $^{13}$C spectrum between atoms representative of different chemical environments makes the $^{13}$C spectrum expecially useful in studying the stereoregularity of the polymer. Whereas the proton spectrum allows observation of dyads and tetrads, the $^{13}$C spectrum extends the knowledge of the stereoregularity to pentad structures. The representative spectrum shown in Figure 2 consists of a number of resonance lines where the triad structures are seen as mm, mr and rr centred lines further split into pentad structures and assigned as follows:-

| Triads | Pentads |
|--------|---------|
|        | m m m m |
| m m    | m m m r |
|        | r m m r |
|        |         |
|        | m m r m |
| m r    | m m r r |
|        | r m r m (not observed in these materials) |
|        | r m r r |
|        |         |
|        | r r r r |
| r r    | r r r m |
|        | m r r m |

A discussion of the information obtained from the $^{13}$C spectrum is to be found later.

## CHAPTER 2

## EXPERIMENTAL PROCEDURES AND RESULTS

### (i) Origin of polymers under examination

The polymers under examination were prepared using a Ziegler catalyst based on milled titanium trichloride activated with an aluminium alkyl chloride. The polymers were made via the route now known as 'gas-phase' polymerisation under commercial conditions. We cannot divulge the route in detail for commercial reasons. However, this thesis is concerned with the effect of racemic units on the solidification process and the origin of the material is therefore not of great significance. Polymer made in this manner is known to contain less than 50 ppm of titanium and less than 100 ppm aluminium. Contamination by hydrocarbon catalyst carrier is reduced to a minimum in this polymerisation process and no hydrocarbon diluent is present at the polymerisation stage, a feature of the more conventional process.

Three whole polymers were chosen and examined initially to establish the stereoregularity of the materials. In addition to the use of NMR, DSC, Infrared spectroscopy and some X-ray crystallography, the polymers were characterised in terms of molecular weight and molecular weight distribution and also flexural modulus.

### (ii) Extraction

As discussed in the introduction the solubility of polypropylene in hydrocarbon solvents was used by Natta (1) to characterise the polymer in terms of crystalline isotactic and amorphous atactic material. Each whole polymer was subjected to continuous extraction by hot solvent to remove the proportion of the polymer which is thought to contain both low molecular weight material and also the less stereoregular polymer. The initial extraction was with boiling n-heptane giving a material referred to as 'heptane insolubles' plus the extract referred to as 'heptane solubles'. One polymer designated as 'C' was also extracted with 100-120°C boiling petroleum and again insoluble polymer was retained for further examination.

(iii)   Instrumental procedures

a)   Nuclear magnetic resonance (NMR)

A Perkin-Elmer R34 super conducting spectrometer system operating at 220 MHz for proton resonance was used to determine the stereoregularity of the polymers.  This instrument is of a conventional continuous wave design and equipped with a variable temperature control probe unit capable of achieving a stable temperature of $140^{\circ}C$ which is that required for this examination.

The racemic dyad (3) contents of the samples were measured using approximately 15% wt/vol solutions of the polymer in a mixture of ortho and para dichlorobenzene. The solvent mixture was prepared as a saturated solution of paradichlorobenzene in ortho dichlorobenzene both to provide a field/frequency lock signal and to ease the dissolution of the polymer.

The 220 MHz spectrum of the whole polymer is shown in fig 1 and indicates (i) the methylene proton resonances present in the polymer as mrm and rrr tetrads as Area A, (ii) the $^{13}C$ satellites (22) of the methyl proton resonance as Area B.  An estimate of the concentration of the racemic centred sequences is made following the method described by Bovey (22).  The area of the resonance from the 'r' centred tetrads is measured and compared with the area of the $^{13}C$ satellite from the isotactic methyl doublet.  It is known that the natural abundance of the $^{13}C$ isomer is 1.1% making this an intensity standard for the isotactic triad content of the polymer under study.

The calculation is performed as follows:-

Area B is one half of the 1.1% of $^{13}C$ satellites for the isotactic content ie 0.55%

Therefore, for a single proton the value is $\dfrac{Area\ B}{3}$

Area A is the resonance assigned to the racemic methylene group

Therefore for a single proton the value is $\dfrac{Area\ A}{2}$

Thus the percentage A in the polymer is $\dfrac{\dfrac{Area\ A}{2}}{\dfrac{Area\ B}{3}} \times 0.55$

The values quoted as % racemic units in table 1  have been obtained following this procedure.

Considerable care is taken to maximise the homogeneity of the magnet. The solutions were heated to 140°C in the spectrometer to achieve maximum resolution. Area A was obtained with the sample spinning rate set at 40 Hz; Area B was obtained with the sample spinning rate set at 30 Hz. These speeds have been found ideal to preferentially remove the spinning side bands of other resonances so that they should not affect the value of the measured areas. The areas under the resonance peaks were measured by planimeter, the average of three readings being taken. The errors concerned with this measurement are dependant upon the instrument, the signal to noise ratio of the spectra obtained and the ability to measure areas by planimeter. These errors are judged to give a ± 10% error on the values obtained.

## (b) Infrared spectroscopy

All infrared spectroscopy was performed on a Perkin-Elmer 580 ratio recording instrument. The design of this spectrometer is such that re-radiation from heated samples is compensated for during the amplification and detection of the signals making quantitative analysis of high quality possible. Repetitive scanning of the spectrum or a portion of the spectrum is a feature of this spectrometer and this mode of operation was used for the measurements of helical contents described. Thus, the time interval between successive scans is known to be constant making kinetic studies feasible on a routine basis.

The samples were prepared as thin films 40-60 μ thick by heating the polymer powder to 180°C for two minutes between 'Fluon' coated steel plates before pressing at 10 ton/cm² on a manually operated hydraulic press followed by rapid cooling to room temperature. The steel plates were coated with 'Fluon' (polytetrafluoroethylene) to assist in releasing the sample from the mould. The thin film samples were mounted between potassium bromide plates and placed in a variable temperature cell capable of temperature control to ± 0.5°C. The unit was then mounted in the sample beam of the 580 IR spectrometer. The spectrometer was set to repeat scan mode

to cover the region 930 - 1075 cm$^{-1}$ with the ordinate set on absorption mode. The sample was melted by raising the temperature to 180$^{\circ}$C for 5 minutes before cooling rapidly to 140$^{\circ}$C and starting to scan the spectrum. This temperature was chosen because the solidification process was neither too rapid or too slow for the measurement of helical growth to be achieved in a reasonable time. The repeat scan took 2 minutes 16 seconds and the percentage helical content was measured for each scan. The method devised to measure the helical content has been in use at I.C.I. for some considerable period and is based on the following:-

Initially, a sample of pure atactic polypropylene was obtained and the absorbance ratio of the absorption band at 825 cm$^{-1}$ and an internal thickness band at 975 cm$^{-1}$ measured. This absorbance ratio was subsequently used as a measure of the atactic content of mixtures of isotactic polymer with atactic polymer present. The helical content of these materials was defined as 100- atactic content. The intensity of the absorption band at 825 cm$^{-1}$ is not easy to measure however in the thin films required for the analysis. There is the possibility of the presence of interference fringe patterns if the parallel surfaces of the films are highly reflective. In addition, as the amount of atactic material is reduced so the more difficult it becomes to measure the intensity of the 825 cm$^{-1}$ absorption band since this is situated between absorption bands due to the helical conformation of isotactic polypropylene. Both these effects can lead to considerable backgrounding errors when measuring intensities and therefore the method was transferred to more suitable absorption bands to measure the helical content. The absorption band observed at 1000 cm$^{-1}$ in isotactic polypropylene is attributed to helical runs of at least 10 monomer units (24) and has been adopted for this measurement after relating to the above work as follows:-

A graph of the ratio $\dfrac{\text{Log}_{10}\ 1_o/_1 1000\ \text{cm}^{-1}}{\text{Log}_{10}\ 1_o/_1\ 975\ \text{cm}^{-1}}$ was

plotted against the ratio

$$\frac{\log_{10} I_o/I \quad 825 \text{ cm}^{-1}}{\log_{10} I_o/I \quad 975 \text{ cm}^{-1}}$$ obtained

from the earlier work as follows:-
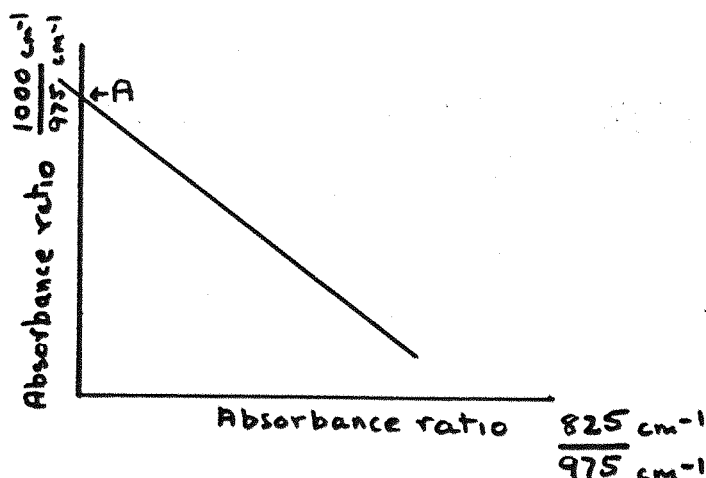


The value of the intercept 'A' is that found for a material containing no atactic polymer i.e. the absorbance ratio

$$\frac{825 \text{ cm}^{-1}}{975 \text{ cm}^{-1}} = \text{zero}$$

The intercept value was found to be 1.06 and was therefore equated to 100% helical by the multiplication factor of 95. Thus, for this work the % helical content is determined from the absorbance ratio

$$\frac{1000 \text{ cm}^{-1}}{975 \text{ cm}^{-1}} \times 95$$

In the above reference it is considered that the 975 cm$^{-1}$ absorption is related to the presence of very short helical runs i.e. 3 or 4 monomer units. It may be better to suggest that the measured helical content is in reality a measure of the increase in long runs of helices. Graphs of the rate of increase in long helical runs with time at 140°C are to be found in the results chapter. Typical infrared spectra are shown in figures 3 and 3[A,B,C], representing the two regions described above.

## Differential scanning calorimetry (D.S.C.)

When changes in the physical state of a material are incurred such as during melting or in transitions from one crystalline form to another, then heat is either given out or absorbed. D.S.C. determines the heat content (enthalpy) of such a

process by measuring the differential heat flow needed to keep
the material of interest and some inert reference sample at the
same temperature throughout a linearly scanned temperature range.
If a change in heat content does occur for the sample during an
experiment then the power output of the system is altered to
compensate for the difference observed between the sample and the
reference. A signal, proportional to the difference between the
heat input to the sample and to the reference, $dH/_{dt}$ m.cal/sec, is
plotted against temperature or time (for isothermal crystallisation).
The system used in the following experiments was calibrated by
making use of a high purity sample of indium whose heat content of
fusion is known to be 6.80 cal./g at the melting point of $156.4^{\circ}$C.

A Perkin - Elmer DSC - 2 differential scanning calorimeter was
used equipped to operate in the range 50 to $725^{\circ}$C. The tables
of results indicate the dynamic crystallisation, remelting and
isothermal crystallisation of the materials examined. Both the
dynamic crystallisation and remelting results were obtained with
a $20^{\circ}$C per minute change of temperature rate. In all experiments
both 'as made' powder and a portion of the film used for the
infrared spectroscopic examination were studied. The samples were
heated to $180^{\circ}$C and held at this temperature for five minutes before
rapidly cooling to $125^{\circ}$C where the polymer was allowed to isotherm-
ally crystallise. The measurements quoted are related to the
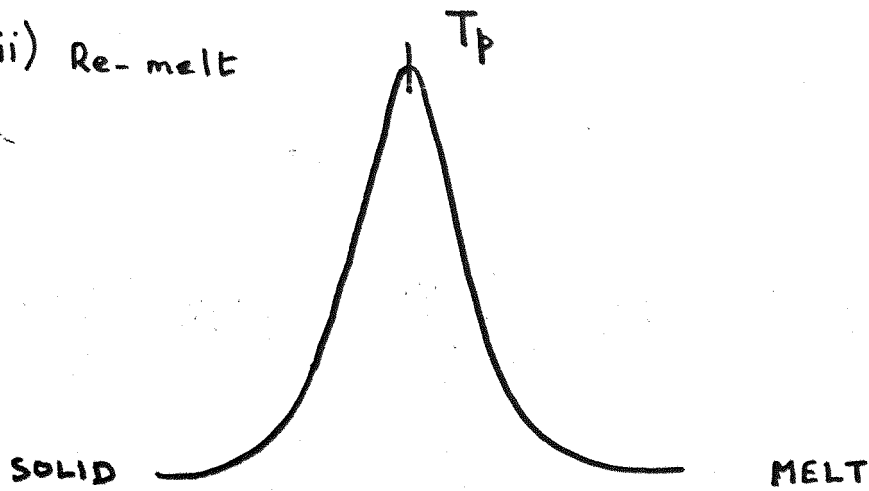crystallisation and melting diagrams as indicated:-
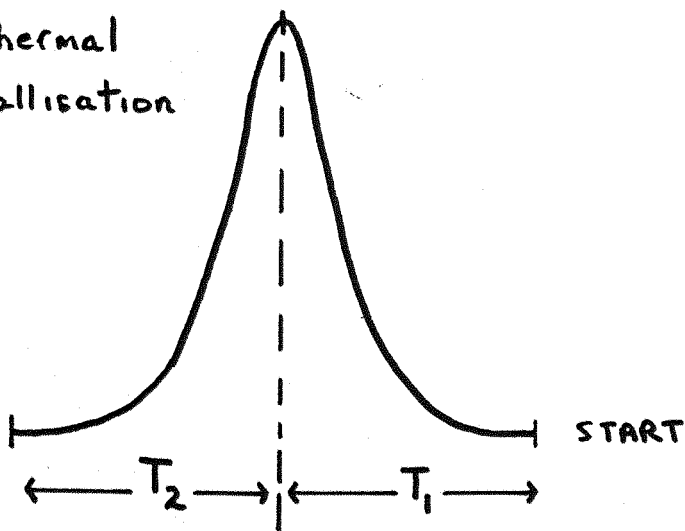
(i) Melt
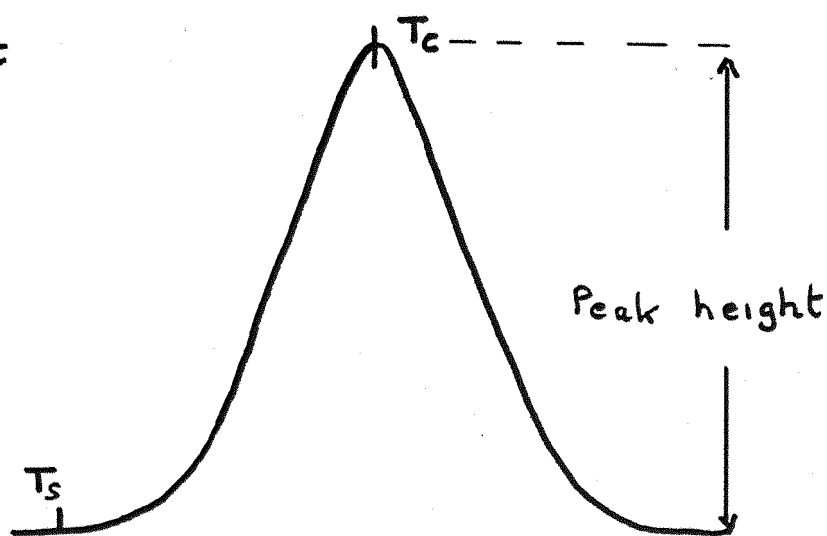


$T_s$   Temperature at which solidification begins

$T_c$   Temperature where crystallisation rate is maximum

ii) Re-melt

$T_p$

SOLID

MELT

iii) Isothermal
crystallisation

START

$\longleftarrow T_2 \longrightarrow | \longleftarrow T_1 \longrightarrow$

$T_1$ Time to maximum rate of crystallisation

$T_2$ Time to complete crystallisation

d)  <u>Molecular weight and distribution</u>,gel permeation
    chromatography. (GPC)

A dilute solution of polymer is washed through a series of columns
tightly packed with porous beads.  Initially, the polymer diffuses
into the pores of the bead then the solvent replaces the polymer
as diffusion out of the bead is induced.  Small polymer molecules
permeate the beads readily and will be involved in many
diffusions in and out of the pores and this will retard their
progress.  Molecules with larger hydrodynamic volume are not so
easily retained in the pores of the beads and are not retarded as
much.  Therefore the larger molecules appear at the end of the
series of columns before the smaller molecules.  The detection
system responds proportionally to the concentration and throughout
the experiments described below a refractive index detector was
used.



Representation of a GPC curve

weight fraction

$10^2$    Log molecular weight    $10^8$
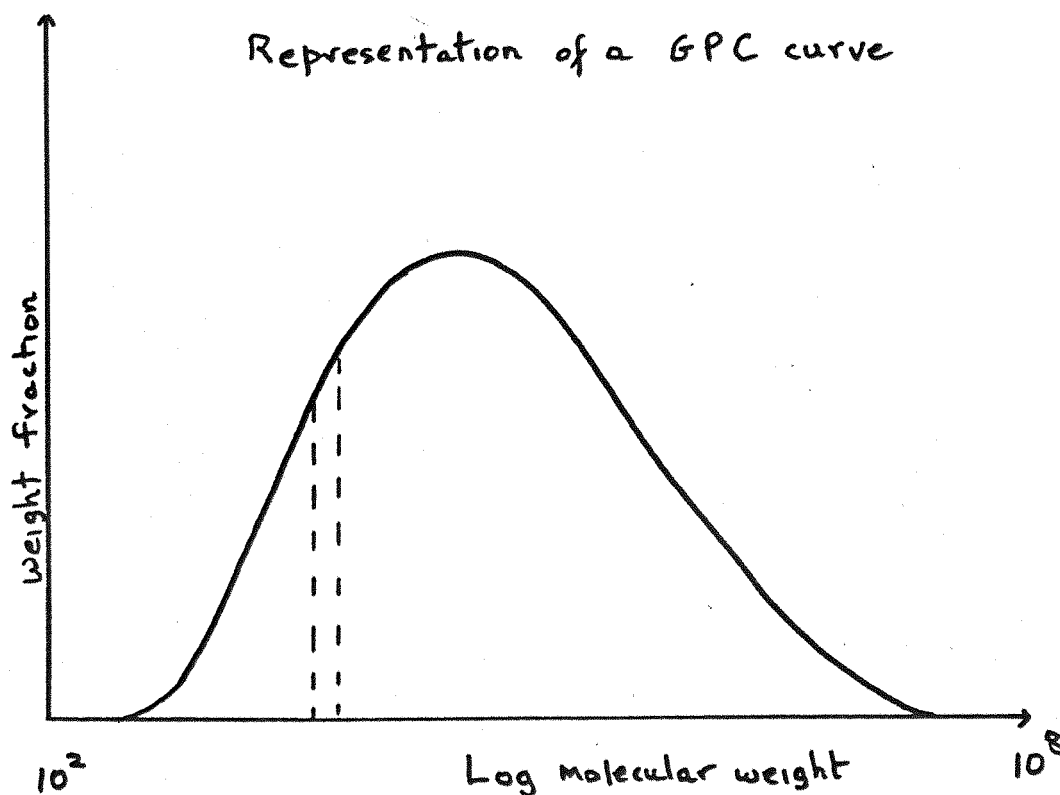
Approximately 100 readings are employed to represent the curve. The area under the curve represents all the molecules present in the sample and shows the distribution of molecular weights. The segment of the curve indicated is equated to a particular elution volume and weight of sample present. The elution volume is measured and calibrated to give the molecular weight. In the case of polypropylene this calibration is achieved from light scattering results on an extremely pure and clean sample of homopolymer. The calibration indicates the molecular weight of the material in the elution volume. The weight of material present in that elution volume is also known. Thus, the weight of sample in each volume is used to construct a table of weights from which the weight average molecular weight is determined. The number average may also be obtained from the total weight of polymer divided by the sum total of molecules for the whole distribution. The sample weight used was approximately 30 milligrams which was dissolved in $\alpha$ -methyl naphthalene to make an approximately 0.25% wt/vol solution. The solution is made at $185^{\circ}C$, a temperature at which it is considered that all inherent crystalline nuclei are destroyed. The column was operated at $165^{\circ}C$ and the results given as weight average $M_w$ number average $M_n$ and the ratio $M_w/M_n$. These are shown in the results section and a typical GPC trace is shown as fig 4. The errors in this method due to base line drift, sample weighing etc are reduced by duplicate runs but must be considered to be $\pm$ 10% for both $M_w$ and $M_n$.

(iv) Presentation of results

i) Nuclear magnetic resonance measurement of the racemic dyad contents of the whole polymer and the insoluble fraction following hydrocarbon semi solvent extraction gave the results presented in table 1. These values indicate the percentage of non isotactic material present in total and make no discrimination as to the placement of such groups in either a molecule which is essentially stereoregular and isotactic or in a molecule which is essentially atactic.

Table 1

Racemic dyad contents %

| Sample | Racemic dyad % |
|---|---|
| A Whole polymer | 1.4 |
| A heptane insoluble | 1.0 |
| A heptane soluble | 12.0 |
| B Whole polymer | 1.9 |
| B heptane insoluble | 1.0 |
| B heptane soluble | 14.0 |
| C Whole polymer | 3.0 |
| C heptane insoluble | 0.8 |
| C heptane soluble | 16.0 |
| C 100–120 petroleum ether insoluble | 0.6 |

ii) Molecular weight measurements by gel permeation chromatography are given in Table 2. The results are quoted as weight average, $M_w$, number average $M_n$ and the distribution average $M_w/M_n$.

Consideration of the values of $M_n$ reveals an inconsistency between the observed whole polymer values and the heptane soluble plus insoluble values after the weight of the soluble material is taken into account. In all cases this value is higher than that observed. For sample A (whole polymer), the observed value is 52,300 $M_n$ and the calculated value is 64,300 $M_n$. Experience gained from the examination of many such samples suggests this inconsistency is frequently encountered. It is considered to be due to the polydisperse nature of the distribution which is only revealed under conditions of higher resolution, i.e. where considerably more than 100 readings are employed to represent the curve.

## Table 2

### Molecular weight measurements

| | Sample | $M_w$ | $M_n$ | $M_w/M_n$ |
|---|---|---|---|---|
| A | Whole polymer | 384,000 | 52,300 | 7.3 |
| A | heptane insoluble | 335,000 | 71,000 | 4.7 |
| A | heptane soluble | 50,000 | 4,000 | 13.6 |
| | | | | |
| B | Whole polymer | 456,000 | 54,000 | 8.5 |
| B | heptane insoluble | 361,000 | 61,000 | 5.9 |
| B | heptane soluble | 26,000 | 4,000 | 7.0 |
| | | | | |
| C | Whole polymer | 570,000 | 79,000 | 7.2 |
| C | heptane insoluble | 600,000 | 103,500 | 5.8 |
| C | heptane soluble | 42,000 | 6,000 | 7.1 |
| C | 100-120 petroleum ether insoluble | 631,000 | 120,000 | 5.3 |

Errors are $\pm$ 10% on the values quoted

Approximately 10% of samples A, B and C was found to be heptane soluble.

A typical curve obtained from the above is labelled as such and is the output from the GPC equipment described in the experimental section.

The extraction procedure has clearly affected the molecular weight distribution with a marked reduction in the low molecular weight tail apparent in all samples.

iii) Differential scanning calorimetry (DSC) results on both the 'as made' powder and as films prepared initially for the infrared examination of helical content formation are presented in tables 3 & 4. The most significant crystallisation parameters, $T_c$ from dynamic crystallisation and $T'$, time to maximum crystallisation rate, from isothermal crystallisation are quoted.

## Table 3

### Differential scanning calorimetry DSC

#### Measurements on powder as made

| | Sample | $T_c(^{o}C)$ | $T'$ mins | NMR % racemic dyads |
|---|---|---|---|---|
| A | Whole polymer | 106.7 | 1.38 | 1.4 |
| A | heptane insoluble | 106.9 | 1.28 | 1.0 |
| B | Whole polymer | 102.9 | 1.85 | 1.9 |
| B | heptane insoluble | 103.9 | 1.60 | 1.0 |
| C | Whole polymer | 114.4 | 0.4 | 3.0 |
| C | heptane insoluble | 107.4 | 1.2 | 0.8 |
| C | 100-120 petroleum ether insoluble | 115.5 | 0.4 | 0.6 |

Errors are $\pm$ 0.2$^{o}$C on the values quoted

## Table 4

### Differential scanning calorimetry

#### Measurements on film

| | Sample | $T_c(^{o}C)$ | $T'$ mins) | NMR % racemic dyads |
|---|---|---|---|---|
| A | Whole polymer | 113.5 | 0.9 | 1.4 |
| A | heptane insoluble | 115.3 | 0.75 | 1.0 |
| B | Whole polymer | 113.5 | 0.95 | 1.9 |
| B | heptane insoluble | 112.5 | 1.15 | 1.0 |
| C | Whole polymer | 110.5 | 1.10 | 3.0 |
| C | heptane insoluble | 110.6 | 0.88 | 0.8 |
| C | 100-120 petroleum ether insoluble | 109.5 | 1.0 | 0.6 |

iv) Annealed crystallinities were determined on pressings of each sample which were slow cooled from 160°C at 6°/hour to develop maximum crystallinity. The crystallinity values were determined by a computer method developed at ICI Plastics Division using diffractometer data.

## Table 5

Annealed crystallinities by X-ray diffraction .

| Sample | | Annealed crystallinities % |
|---|---|---|
| A | Whole polymer | 77 |
| A | heptane insoluble | 77.5 |
| B | Whole polymer | 75 |
| B | heptane insoluble | 76.5 |
| C | Whole polymer | 70.5 |
| C | heptane insoluble | 73.5 |
| C | 100-120 petroleum ether insoluble | 75.5 |

Errors involved amount to $\pm$ 0.5% on these particular values

The data presented in table 5 show that the annealed crystallinity increases after extraction with hydrocarbon semi-solvent. This is particularly noticeable in sample C.

The method used is based on Rulands (25) basic rules but with adjustments made to base line determinations. Scatter contributions come from two recognisable sources, air scatter and incoherent scatter. The air scatter is measured and the incoherent scatter calculated; addition of these two effects gives rise to the adopted base line as shown in diagram.
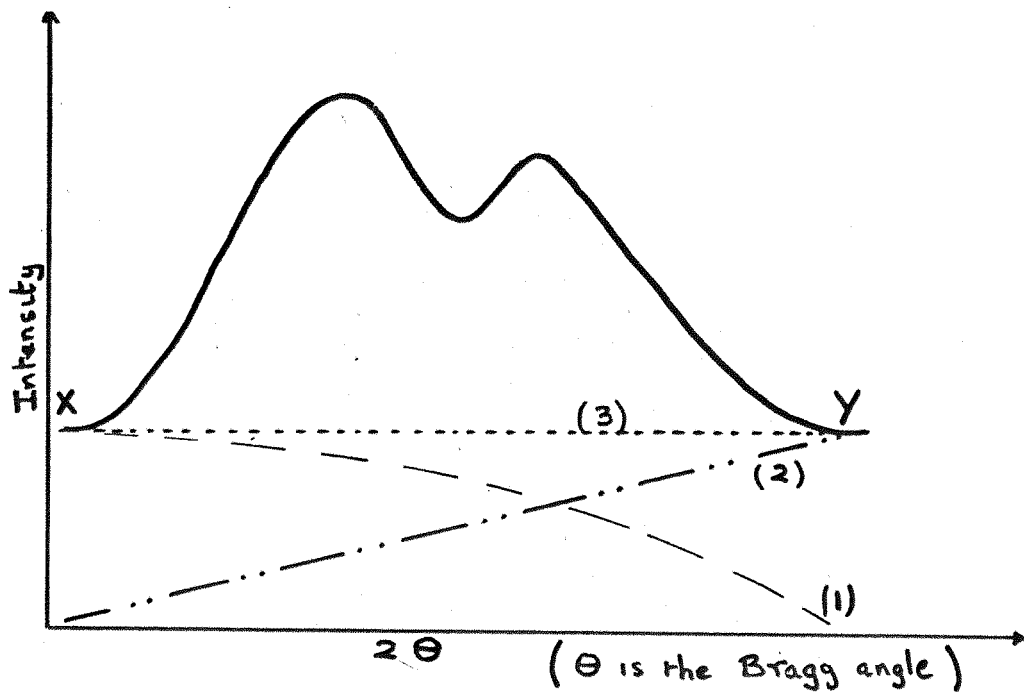
(1)   is the measured air scatter

(2)   is the calculated incoherent scatter

(3)   is the adopted base line

X     is usually below $10^{\circ}$

Y     is usually taken to be $38^{\circ}$

It is assumed that everything above the line (3) between points X and Y is the scatter from the sample. The scatter from totally amorphous regions is drawn in from the scatter obtained from an atactic amorphous sample. In addition the scatter observed from molten isotactic polymer was also used in combination with the atactic amorphous scatter to determine the amorphous curve as shown in the figure representing the scatter from essentially isotactic polypropylene. This curve is fitted under the experimental curve and the crystallinity determined as follows:-

$$\text{Wt \% crystallinity } \chi = \frac{C_{\text{crystalline area}}}{C_{\text{crystalline}} + k\,A_{\text{amorphous}}}$$
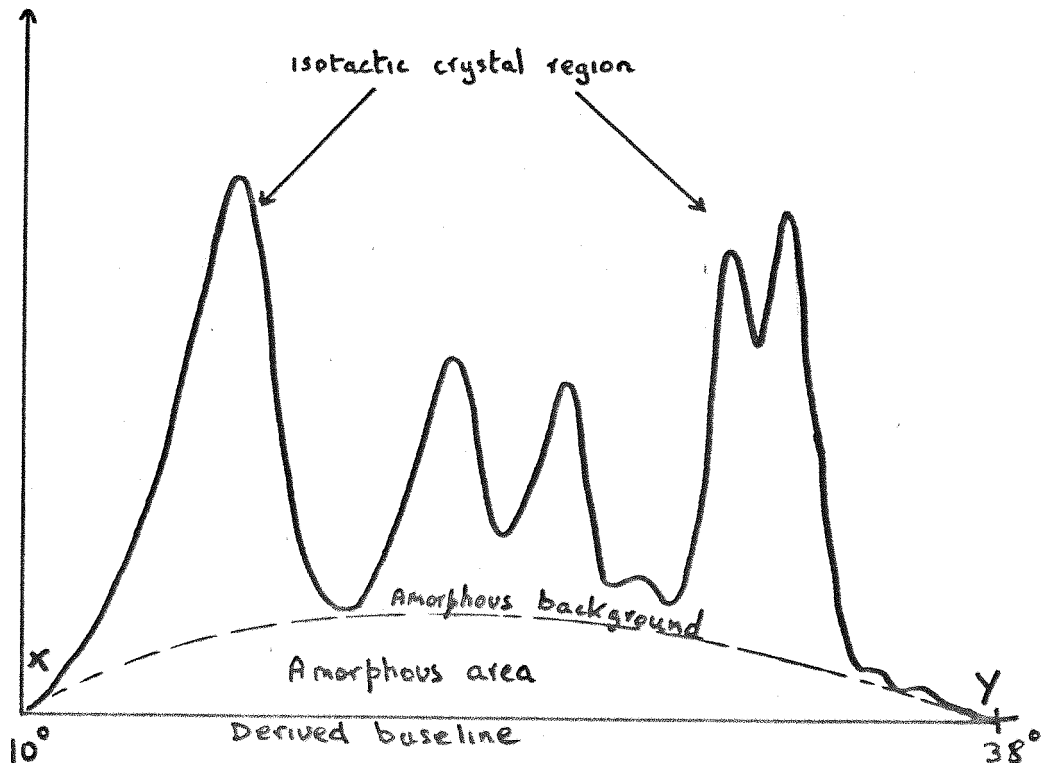
is a factor different for each polymer type and related

o the density/crystallinity relationship observed when the specific volume is plotted against the crystallinity measured.
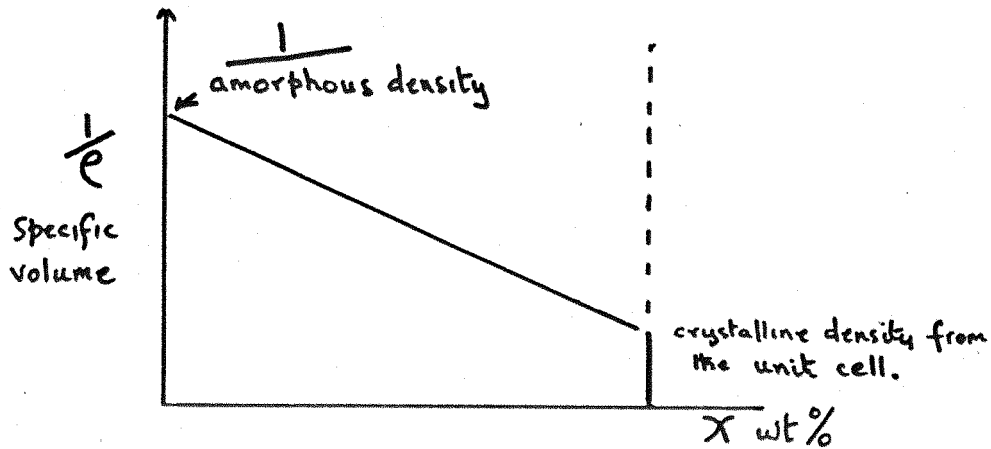


The errors in this procedure have been calculated as $\pm$ 5%

Figure representing polypropylene diffraction pattern and analysis

The errors quoted for the x-ray data appear to be inconsistent in that the result of plotting specific volume against crystallinity has an error of $\pm$ 5% whereas the annealed crystallinity which requires the former result, has an error of $\pm$ 0.5% incorporated. Experience of crystallinity measurements shows that the reproducibility errors may be restricted to the $\pm$ 0.5% quoted, i.e. those particularly concerned with area measurement and delineation of backgrounds. Since the same method and backgrounds are used for these samples and the resulting values cover only a small numerical range, the relative values are considered to be within the errors quoted. The estimation of all errors involved in the x-ray analysis of heterogeneous systems such as polymers is a formidable task and has not been attempted here.

## Infrared determination of the rate of helical formation on cooling from the melt

As previously described, the helical content (%) of the various whole and extracted samples when solidified under isothermal conditions was determined by measurement of the ratio of the peak heights of the $\frac{1000 \text{ cm}^{-1}}{975 \text{ cm}^{-1}}$ absorption bands.

The following tables indicate the helical contents measured at identical time intervals $H_t$, the final helical content $H_\infty$ plus the values $H_\infty - H_t$ and $\frac{d(H_\infty - H_t)}{dt}$ required to comment on the rates of helical formation.

Table 6

| Sample A  (whole) | measured at the stable temperature of 140°C | | |
|---|---|---|---|
| $H_t$ | $H_\infty - H_t$ | $\dfrac{d\,(H_\infty - H_t)}{dt}$ | $H_\infty = 74$ |
| 19 | 55 | 5.51 | |
| 26 | 48 | 9.51 | |
| 38 | 36 | 15.95 | |
| 50 | 24 | 11.32 | |
| 61 | 13 | 6.67 | |
| 67 | 7 | 5.31 | |
| 70 | 4 | 3.19 | |
| 72 | 2 | 1.56 | |
| 73 | 1 | 0.81 | |

## Table 7

| Sample A | (heptane insoluble) | measured at the stable temperature of $140^{\circ}C$ | |
|---|---|---|---|
| $H_t$ | $H_\infty - H_t$ | $\dfrac{d(H_\infty - H_t)}{dt}$ | $H_\infty = 72$ |
| 42 | 30 | 60.8 | |
| 65 | 7 | 5.0 | |
| 68 | 4 | 2.5 | |
| 69 | 3 | 1.4 | |
| 70 | 2 | 1.0 | |
| 71 | 1 | 0.8 | |

## Table 8

| Sample B | (whole polymer) | | |
|---|---|---|---|
| $H_t$ | $H_\infty - H_t$ | $\dfrac{d(H_\infty - H_t)}{dt}$ | $H_\infty = 68$ |
| 19 | 49 | 3.8 | |
| 25 | 43 | 6.9 | |
| 31 | 37 | 7.0 | |
| 39 | 29 | 6.8 | |
| 46 | 22 | 6.5 | |
| 51 | 17 | 4.8 | |
| 55 | 13 | 4.0 | |
| 59 | 9 | 3.2 | |
| 62 | 6 | 2.3 | |
| 64 | 4 | 1.6 | |
| 65 | 3 | 1.3 | |
| 67 | 1 | 0.8 | |

## Table 9

| Sample B (heptane insoluble) | | | |
|---|---|---|---|
| $H_t$ | $H_\infty - H_t$ | $\dfrac{d(H_\infty - H_t)}{dt}$ | $H_\infty = 72$ |
| 44 | 28 | 25.9 | |
| 63 | 9 | 10.5 | |
| 68 | 4 | 4.6 | |
| 71 | 1 | 1.6 | |

## Table 10

| Sample C (whole polymer) | | | |
|---|---|---|---|
| $H_t$ | $H_\infty - H_t$ | $\dfrac{d(H_\infty - H_t)}{dt}$ | $H_\infty = 66$ |
| 18 | 48 | 5.3 | |
| 26 | 40 | 7.7 | |
| 34 | 32 | 9.2 | |
| 43 | 23 | 7.6 | |
| 49 | 17 | 5.4 | |
| 54 | 12 | 4.3 | |
| 58 | 8 | 3.7 | |
| 62 | 4 | 3.0 | |
| 64 | 2 | 1.7 | |
| 64 | 2 | 1.1 | |

## Table 11

| Sample C | (heptane insoluble) | | |
|---|---|---|---|
| $H_t$ | $H_\infty - H_t$ | $\dfrac{d\,(H_\infty - H_t)}{dt}$ | $H_\infty = 68$ |
| 23 | 45 | 12.3 | |
| 34 | 34 | 9.8 | |
| 43 | 25 | 8.3 | |
| 50 | 18 | 6.8 | |
| 57 | 11 | 5.2 | |
| 61 | 7 | 3.8 | |
| 65 | 3 | 2.2 | |
| 66 | 2 | 1.5 | |
| 67 | 1 | 1.0 | |
| 67 | 1 | 0.6 | |

## Table 12

| Sample C | (Pet-ether 100-120 insoluble) | | |
|---|---|---|---|
| $H_t$ | $H_\infty - H_t$ | $\dfrac{d\,(H_\infty - H_t)}{dt}$ | $H_\infty = 74$ |
| 62 | 12 | 14.5 | |
| 70 | 4 | 4.1 | |
| 71 | 3 | 1.6 | |
| 73 | 1 | 0.7 | |
| 73 | 1 | 0.1 | |

Based on the data given in the tables (1) to 12), three representative series of graphs have been plotted. The first series indicates the increase in helical content (%) with time and are labelled graphs 1 to 3. The second series is the plot of $H_{\infty} - H_t$ with the time interval, t, from which the tangent to the curve at each data point can be determined. These graphs are labelled 4 to 6. The third series of graphs (7 to 9) are those plotted as the $\log \dfrac{d\,(H_{\infty} - H_t)}{dt}$ against $\log\,(H_{\infty} - H_t)$. The slope of the line determined from this plot indicates the rate of production of the helical conformation. These values are indicated in Table 13.

Table 13

| Sample | Slope $\dfrac{d\,(H_{\infty} - H_t)}{dt}\Big/ H_{\infty} - H_t$ |
|---|---|
| A (whole) | 0.74 |
| A (heptane insoluble) | 1.35 |
| B (whole) | 0.88 |
| B (heptane insoluble) | 0.84 |
| C (whole) | 0.55 |
| C (heptane insoluble | 0.72 |
| C (100-120 pet-ether insoluble) | 1.46 |

An indication of the influence that molecular weight may have when considering the role of racemic dyads in determining the ultimate crystallinity is shown in graph 10. The data from which this curve is derived is to be found in tables 2 and 5 of this chapter.

The following table gives the relationship observed between the racemic dyad content and the time taken to achieve 80% of the final helical content.

Table 14

| Sample | Racemic dyad(%) | Time to 80% final helical content (mins) |
|---|---|---|
| A (whole) | 1.4 | 11 |
| A (heptane insolubles) | 1.0 | 4 |
| B (whole) | 1.9 | 15 |
| B (heptane insolubles) | 1.0 | 4 |
| C (whole) | 3.0 | 15 |
| C (heptane insolubles) | 0.8 | 10 |
| C (Pet-ether 100-120 insolubles) | 0.6 | 2 |

These results are plotted in graph 11 to indicate the influence of racemic dyads on the rate of helical growth.

## Flexural modulus

The flexural modulus of polypropylene is determined by a three point method. A bar of polymer with a rectangular cross section is prepared by compression moulding at $250^{\circ}C$. The polymer is allowed to cool to room temperature over a 10 minute period and is subsequently annealed at $130^{\circ}C$ for 2 hours before cooling to room temperature over a further 12 hour period. The rectangular bar of polymer rests on two supports and the load is applied by means of a loading nose situated halfway between the two supports.
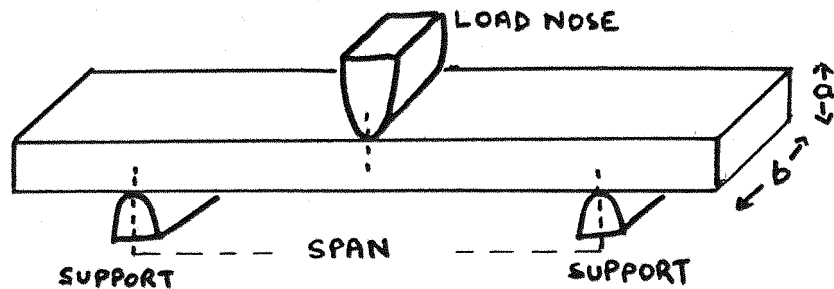


The flexural modulus $(M_F)$ is given by the following equation:-

$$M_F \; (\text{GN/m}^2) = \frac{(\text{Span (mm)})^3 \, (\text{max. slope of the stress/strain curve})}{4 \, (\, (\text{width})(b)_{mm})(\text{thickness } (a)_{mm})^3 \,)}$$

An 'Instron' testing machine is used to load the sample. The Instron possesses a constant rate of crosshead speed and is equipped with a deflection measuring device. The load is applied to the polymer bar at a specific crosshead rate and load/deflection data is obtained. The load/deflection curve so obtained is used to measure the maximum slope value required to calculate the flexural modulus.

# CHAPTER 3

## DISCUSSION OF RESULTS

The work described in this thesis was initiated to make observations on the influence of non-stereoregular units on the solidification process of essentially isotactic polypropylene homopolymer. The three polymers used for this work were made by the gas phase process. The solvent extraction used to remove the less stereoregular material was carried out on the "as made" powder and it is worth noting that the DSC measurements show that the structure of the original powder is changed very little by the extraction process, for example the melting point of the powder alters very little after the extraction as measured by the dynamic $T_c$ value. The melting point of the powder is lower in all cases than that observed after the sample is melted and subsequently annealed. Previous experience shows that "as made" homopolymer powders have crystallinities close to 50%. This value taken alone is not of much concern especially since in the commercial world the usefulness of a polymer is dictated by its physical properties after it has been fabricated. However, it is interesting to know that some other polymers "as made" have rather different powder crystallinities ie polytetrafluoroethylene with a crystallinity in excess of 95% and high density polyethylene at about 80%.

The early stages of polymerisation play a very significant role in deciding the morphology of the "as made" powder. The study of the nascent morphology of polyolefins is an area which has provided surprises, interest and speculation. Perhaps the first significant approach to this area of study was that of Wunderlich (26) in which he comments that in the case of a crystallisable polymer it is possible to bypass the random coil conformational state and proceed directly from monomer to bulk crystalline polymer. Nascent morphology is produced when the polymerisation takes place in a non solvent and at a temperature below the melting point of the final crystalline product. The polymerisation

of tetrafluoroethylene by the normal emulsion process
obviously fulfills both stated conditions and nascent
morphology results. It would appear that extended chain
polymerisation (26A) occurs and a highly ordered crystalline
product is obtained. Subsequent heating above the melting
point alters this morphology greatly leading to a reduction
in the crystallinity from the original 95% to 60-70% plus
a transformation of extended chain morphology to that of a
chain folded morphology. Heterogeneous catalysis of ethylene
to form high density polyethylene also fulfills the condition
for nascent morphology and again the extended chain form is
present to a fairly high proportion (27). However, in this
case the crystallinity falls very short of 100%, more often
observed near 80%. Perhaps this is due to limited solubility
of short segments of the polymerising chain in its own
monomer. Again subsequent melting of the nascent polymer
results in a change to the chain folded morphology and a
consequent reduction in both crystallinity and melting
point. The gas phase polymerisation of propylene would also
seem to give rise to nascent morphology. However, it has
been indicated (28) that the temperature at the polymerisation
site may be high due to the exothermic nature of polymerisation
with $\Delta H_p \approx$ -104.68 K Joules for both polyethylene and
polypropylene(29, 30). Thus, the polymer produced at the
polymerising site could be in or close to the melt. A
review of the evidence for nascent morphology is given by
Marchessault, Fisa and Chanzy (31) and also by Wunderlich
(32) where the influence of nucleation is considered on
nascent morphology. It has been concluded from such studies
that for polyethylene the proportion of extended chain
crystallites present depends on the polymerisation conditions.
There is apparently no evidence for an extended chain form
of nascent polypropylene in nascent morphology (although
Morrow (33) has commented upon the possibility of this
modification) and this may well be why the lower
crystallinity is observed in "as made" powder. Although
much remains to be studied, a number of factors are known to
influence the morphology of "as made" polymer which include
the catalyst system, the presence or otherwise of solvent

and whether or not the forming polymer is soluble in its own monomer and also the temperature attained at the polymerisation site.

The extraction of "as made" polymer powder removes the less stereoregular polymer as indicated in table 1 but as previously mentioned, the extraction makes little change to the crystalline portion. The nature of the extracted material is therefore a question worthy of consideration. In all cases the racemic dyad concentration of the soluble material is approximately one order of magnitude higher than the original unextracted polymer. The assignment of the resonance peaks observed in the proton ($^1$H) spectrum is common knowledge but is indicated in figure 1, based on the work of Heatley (34) and confirmed by Ferguson (35).

Most of the extractable material is still the isotactic form but the non isotactic content can be assigned to mrm and rrr with a smaller contribution likely from mrr and rrm sequences. It is likely therefore that the interference of isotactic sequences following malfunction of the catalyst results in either mistakes giving rise to mrm and mrr tetrads or in a more serious breakdown of stereospecificity to give rrr tetrads. Even after extraction and with a subsequent drop in the racemic dyad concentration, the residual insoluble polymer still contains these same sequences. It is probable therefore that the extraction process removes primarily the available non stereoregular polymer plus a proportion of low molecular weight isotactic polymer. In total, less than 10% of the original "as made" polymer. This material must be present to a large extent outside the crystalline regions of the "as made" polymer powder. Since the racemic dyad concentration does not fall to zero two assumptions can be made. Either the non isotactic sequences can cocrystallise with the isotactic runs or that they are protected from solvent attack by being an integral part of the morphology. Any long runs of an atactic nature are most unlikely to form part of a crystalline region due to their inability to form helices of the necessary dimensions. Single isolated mrm or mrr (m) units may still be captured by the crystalline regions but find themselves

at the crystal interfaces. These units will therefore be resistant to attack by solvent during the extraction process. These views are strongly supported by the $^{13}$C NMR spectrum (fig 2). The extracted polymer shows a decrease in the rrrr pentads relative to the mmrm sequence (the isolated fault) showing that there may well be two types of non stereoregular materials with the more atactic species being preferentially attacked by the solvent. This latter material is unlikely to take part in the crystallisation process at all and probably will have little effect on the rate at which crystallisation takes place in the more stereoregular species. The more simple sequences mmrm and mrrm could be much more important in determining both rate and extent of crystallisation since they may well be incorporated in an otherwise isotactic sequence. The consequence of this view is to believe that the catalyst has at least two different active sites for polymerisation. One gives rise to the atactic material which is extracted by solvents whereas another site is stereospecific to a very large degree giving the major isotactic species.

The effect of removing the soluble fraction on the ultimate crystallinity can be seen in table 5. The polymer was examined as stated in the form of an annealed film. The polymer powder is melted and then annealed to give a suitable specimen for X-ray analysis. In all three instances the ultimate crystallinity increases with the removal of the extractable portion but noticeably more so when a higher boiling solvent is used (sample C) and the racemic dyad content reduced to a lower value. As discussed earlier, the crystallisation of polypropylene is dependent on the extension of the runs of helices and the alignment of isotactic helical molecules in space to form a three dimensional network, and then the registration of this network into lamellar units. Since the formation of helices is the first stage in achieving good crystallinity a study of the rate at which helices form is also an important aspect of this work.

The helical content of these polymers as they solidify
from the melt has been monitored by a study of the
infrared spectrum as shown previously. The racemic dyad
concentration generally affects the final helical content
but the scatter on the results as indicated by graph 12
suggests that other factors may also play a significant
part in the solidification process. As part of the
determination of the rate of helical formation, the time
taken to reach 80% of the achievable value has been
plotted against the racemic dyad content, graph 11.
Again, the generalisation can be made that the higher the
racemic dyad content then the longer the time taken to
reach 80% of the final helical value. The rate at which
helices are formed is given in table 14 and this is seen
to increase as the racemic dyad concentration falls.

As already discussed, crystallisation depends
primarily on the ability of molecular chains to form the
necessary helices. Thus, a useful correlation should be
observed between racemic dyad content and the annealed
crystallinity. This correlation is presented in
graphical form (10). At a first glance there is
apparently only a superficial correlation. However, if
the samples are separated one from another the correlation
is much more certain. There is a further refinement
necessary after which the graph reveals the significance
of this work. The molecular weights of samples A, B & C
are different. Sample A is approximately 350,000;
sample B is approximately 400,000; sample C is
approximately 600,000. When these differences are taken
into account the correlation between structural perfection
and achievable crystallinity becomes clear. The higher
the molecular weight the lower the achievable
crystallinity. Thus, two parameters contribute to the
solidification process, the racemic dyad concentration
and the molecular weight both of which must be taken into
account when further examination of the physical properties
and behaviour of the polymer during fabrication is
necessary. The ultimate crystallinity is achieved only
very slowly for high molecular weight material, ie the

the process is governed by kinetics rather than
thermodynamics.

As a further examination of the whole polymer reveals
the modulus (flexural) shows an increase as the racemic
dyad content falls. This observation is entirely
consistent with the experience gained from the examination
of a considerable number of polymer samples carried out
during normal commercial evaluation of polypropylene.
The author of this thesis has made use of this observation
to devise and evaluate a test method making use of
racemic dyad contents measured by high resolution proton
NMR and the flexural modulus. Such a correlation is
displayed in graph 13. Neither the flexural modulus test
nor the high resolution NMR method can be considered
suitable for quality control close to the production plant
environment. In the first instance the time taken to
prepare a suitable sample is excessive and in the NMR case
the delicate instrumentation, the sample size (usually
less than 0.5 gram) being an insignificant size per batch
of polymer plus the necessity to dissolve the sample in a
suitable solvent all make this form of examination
untenable. However, if the assumption is made that the
flexural modulus reflects the motional characteristics of
the material and that the presence of racemic dyads
increases this motion it might be possible to use a wide
line NMR method which measures the motion of molecular
chains. A very simple NMR spectrometer has been produced,
the Newport Quantity Analyser, which can observe the
dipolar interactions of protons in a solid and overcomes
many of the problems posed for plant operation. The
bandwidth of this resonance is reduced as the mobility of
the material increases, ie a tendency to average the
dipolar interactions toward zero. Gating of the resonance
is possible so that the relatively mobile fraction can be
observed more or less separately from the relatively more
rigid component. These values give a good correlation
with first of all the racemic dyad content measured by
solution high resolution NMR and secondly with the
measured flexural modulus of the polymer under examination,

graphs 12 & 13. The fall in modulus with increasing
racemic dyad concentration must relate to their effect
on the solidification process giving rise to non-
crystallisable regions and/or defects in the crystalline
areas. Since the major influence on the modulus of
polymeric materials is to be found in the rigidity of the
crystalline arrays, the presence of defects (stereo-
irregularities) within these areas seems to offer an
explanation.

# CHAPTER 4

## CONCLUSION

Three different polymers were extracted with
n-heptane giving soluble and insoluble fractions.  The
low molecular weight and atactic material was extracted
from each polymer leaving three insoluble materials with
slightly disparate molecular weights, each having a low
racemic dyad content and lower than the whole polymer in
each case.

The crystallisation behaviour of the insoluble
fractions was studied and it was observed that the
ultimate crystallinity decreased  with increasing molecular
weight in both the extracted and whole polymers.  This
could be a kinetically controlled observation rather than
a thermodynamic one but if so one would have expected the
low molecular weight portion to have increased the
crystallinity process whereas it would appear not to do so.
Perhaps the molecular weight is not so important since the
molecular weight of the three polymers is not grossly
different.  It will be seen below that many properties of
the three polymers vary from one to another.  Unfortunately,
two parameters vary between them coincidently.  That is
the molecular weight of the polymers $A < B < C$  and at
the same time the racemic dyad concentration varies.
However, the latter varies very little in the whole
polymer and certainly less than it does as a consequence
of extraction.  The problem is to describe the variation
in the property observed as a consequence of either
molecular weight or racemic dyad concentration or both.
The molecular weight of polymers $A \rightarrow C$ changes from $M_w$
of $384000 \rightarrow 570000$ or $M_n$ $52000 \rightarrow 79000$  with a fairly
constant dispersivity.  Thus, the molecular weights are
high and relatively constant and it was difficult to
explain all the observations simply on this basis.

Let us therefore consider the role of the racemic
dyad concentration.  Reducing the racemic dyad
concentration to a very low level by prolonged extraction
increases the rate of helix formation compared with the
whole polymer even though the molecular weight rises and

the plasticising effect of small polymer fragments is
drastically reduced. Lowering the racemic dyad
concentration does not appear to change the ultimate
degree of crystallinity a great deal. One would have
expected that long runs of meso units (the basic unit
of the isotactic chain) might have encouraged crystall-
isation by facilitating the extension of $3_1$ helical
sequences in the first stage of the crystallisation
process. One would also have expected as reported
above that removal of low molecular weight material
would discourage molecular mobility and hence later steps
in the crystallisation process. As is often the case
neither expectation is realised.

The property known as the flexural modulus is vital
to the commercial aspects of polypropylene. It appears
that when comparing a wide range of polymers all produced
by the gas phase process and having a range of racemic
dyad concentrations that an increase in the latter can be
linearly related to a fall in the flexural modulus. The
conventional view is to relate this property to distortion
of the non crystalline material in the polymer. The
degree of crystallinity changes very little with
considerable variation in the racemic dyad concentration
but if there is a correlation it is likely that the
racemic dyad concentration and crystallinity are
inversely related. As a consequence one might expect
that as the racemic dyad concentration falls the
flexural modulus would rise and this is indeed what is
found.

It is quite clear that progress in this project is
very much in its early stages. We urgently need detailed
information on the structure of the disordered part of
the polymer and subsequently its role in controlling
properties. It is well established that all the
classical methods available for structure determination
are incapable of solving this problem. Solid state high
resolution NMR appears to be an exciting new prospect.
The technique is difficult, the analysis of data still

not rigorous but the preliminary results are
encouraging. Over the next few years the type of problem
described in this thesis may well be solved by this means.
The author is involved in this new venture [36,37] and
two new contributions to the literature are included as
appendices A and B.

This thesis demonstrates the need for further
examination of the influence of the disordered zones on the
mechanical properties of polypropylene. This is in progress
and a paper related to this subject will be published at a
later date.

# REFERENCES

1) G.Natta, P.Pino, P.Corradini, F.Danusso, E.Mantica, G.Mazzanti and G.Moraglio.
J. Amer. Chem. Soc. $\underline{77}$, 1708, (1955)

2) G.Natta. Atti. Accad. Nazl. Lincei, Memorie (8), $\underline{4}$, 61, (1955)

3) F.A.Bovey. 'High resolution NMR of macromolecules' Academic Press, 1972.

4) G.Natta, P.Corradini, I.W.Bassi, L.Porri. Atti. Accad. Nazl. Lincei Rend Classe Sci.Fis.Mat.Nat. $\underline{24}$, 121, (1958)

5) G.Natta, I.Pasquon, A.Zambelli, G.Gatti. J.Polymer. Sci. $\underline{51}$, 387 (1961)

6) C.A.Emeis, F.J.Reinders, E.Drent. Solid state communs. $\underline{16}$, 239 (1975)

7) G.Natta, I.Pasquon, A.Zambelli, G.Gatti. J.Polymer Sci. $\underline{51}$, 399, (1961)

8) A.Zambelli, I.Pasquon, G.Natta. Makromol. Chem. $\underline{112}$, 160, (1968)

9) A.D.Caunt. Specialist Periodical Report, Catalysis, Vol 1. London Chemical Society, 1977

10) P.Cossee. 'The stereochemistry of Macromolecules' Vol 1. Marcel Dekker N.Y 1967

11) D.R.Armstrong, C.G.Perkins, J.J.P.Stewart. Rev. Roum.Chim. $\underline{19}$, (11), 1695, (1974)

12) A.Zambelli, 'Co-ordination Polymerisation' Academic Press, 1975

13) G.Natta, M.Farina, M.Peraldo.
    Chim. Ind.(Milan) 42, 255, (1960)

14) T.Miyazawa, T.Ideguchi.
    J.Polym.Sci. B1, 389 (1963)

15) A.Zambelli, M.G.Giongo, G.Natta.
    Makromol.Chem. 112, 183, (1968)

16) E.J.Arlman, P.Cossee.
    J.Catalysis 3, 99, (1964)

17) J.C.Woodbrey. 'The stereochemistry of
    Macromolecules' Vol 3, Marcel Dekker, (1968)

18) R.C.Ferguson, Trans. N.Y. Acad.Sci.29, 495 (1967)

19) F.Heatley, R.Salovey, F.A.Bovey.
    Macromolecules 2, 619, (1969)

20) A.Zambelli, A.L.Segre.
    J.Polym.Sci. part B, 6, 473, (1968)

21) F.Heatley, A.Zambelli.
    Macromolecules 2, 618, (1969)

22) F.Heatley, R.Salovey, F.A.Bovey.
    Macromolecules 2, 619 (1969)

23) Yu.V.Kissin, V.I.Tsvetkova, N.M.Chirkov.
    European Polymer Journal, 8, 529, 1972.

24) Yu.V.Kissin, L.A.Rishina.
    European Polymer Journal, 12, 757, 1976.

25) W.Ruland. Acta Cryst. 14, 1180, 1961.

26) B.Wunderlech. Fortschr. Hochpolym.
    Forsch 5, 568, 1968.

26A) F.J.Rahl. J.Polym.Sci. A-2 10, 1337, 1972

27) B.Wunderlech, C.M.Cormier.
    J.Polym.Sci. A-2, 5, 987, 1967

28) J.Y.Guttman, J.E.Guillet. Macromolecules 3, 470, 1970

29) G.S.Parks, H.P.Mosher.
J.Polym.Sci. Part A1,   1979, 1963

30) V.E.Ostrovskii et al.   Dokl. Adad.Nauk SSSR,
184, 103, 1969

31) R.H.Marchersault, B.Fisa, H.D.Chanzy.
CRC critical reviews in Macromolecular
Science, 315, 1972 (October)

32) B.Wunderlich.  Macromolecular Physics Vol 2
(crystal nucleation, growth and annealing)
Acad.Press 1976  p.282

33) D.R.Morrow.  J.Macromol.Sci.Phys $\underline{3}$, 53, 1969

34) F.Heatley, A.Zambelli.  Macromolecules $\underline{2}$,
No 6, 618, 1969

35) R.C.Ferguson.  Macromolecules $\underline{4}$, No 3, 324, 1971

36) A.Bunn, M.E.A.Cudby, R.K.Harris, K.J.Packer, B.Say
J.Chem.Soc.Chem.Comm. 15, 1981

37) G.Baliman, M.J.S.Burgess, R.K.Harris, A.G.Oliver,
K.J.Packer, B.J.Say,  S.F.Tanner, R.W.Blackwell,
L.W.Brown, A.Bunn, M.E.A.Cudby and J.W.Eldridge.
Chem.Phys. $\underline{46}$, 469, 1980
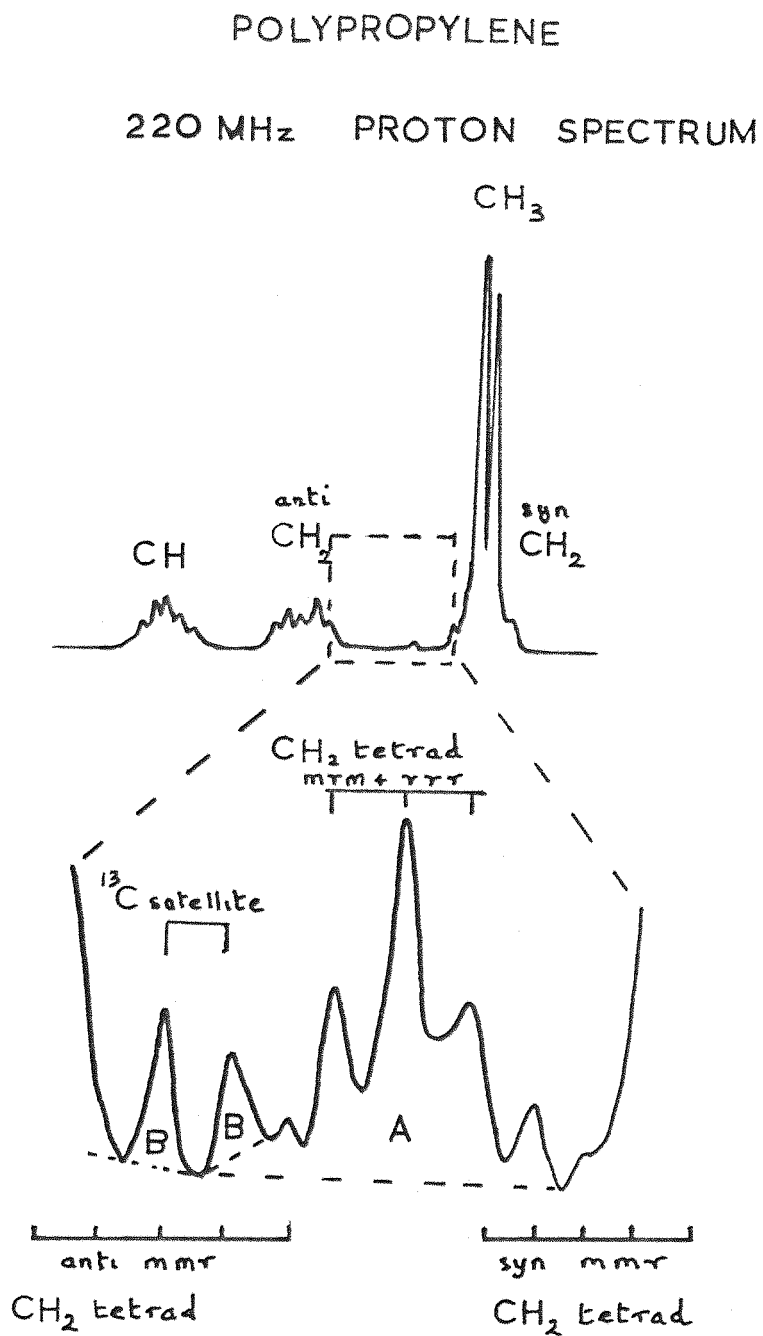
FIGURE I.

REPRESENTATION OF $^{13}C$ SPECTRUM
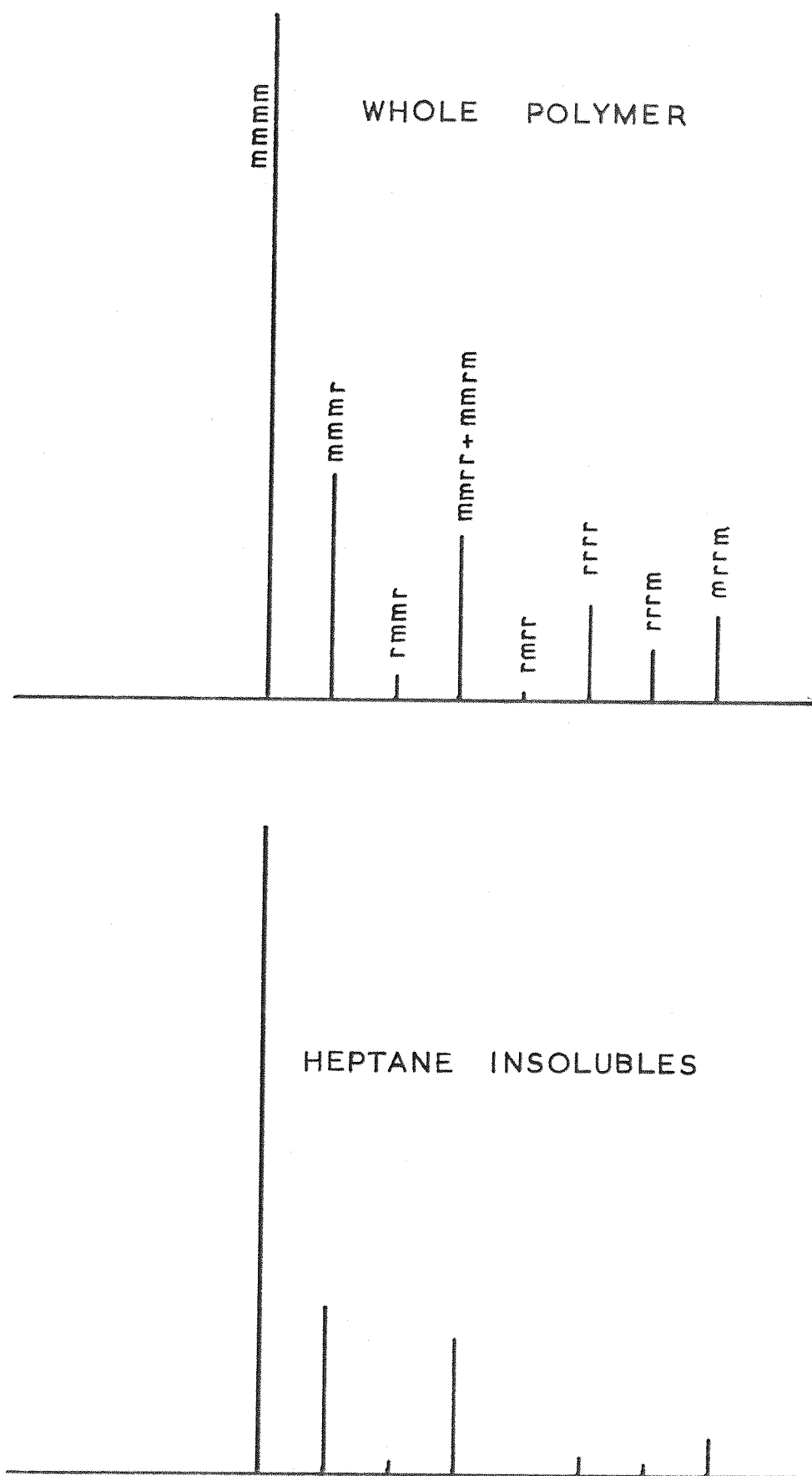


FIGURE 2.

# INFRARED SPECTRUM
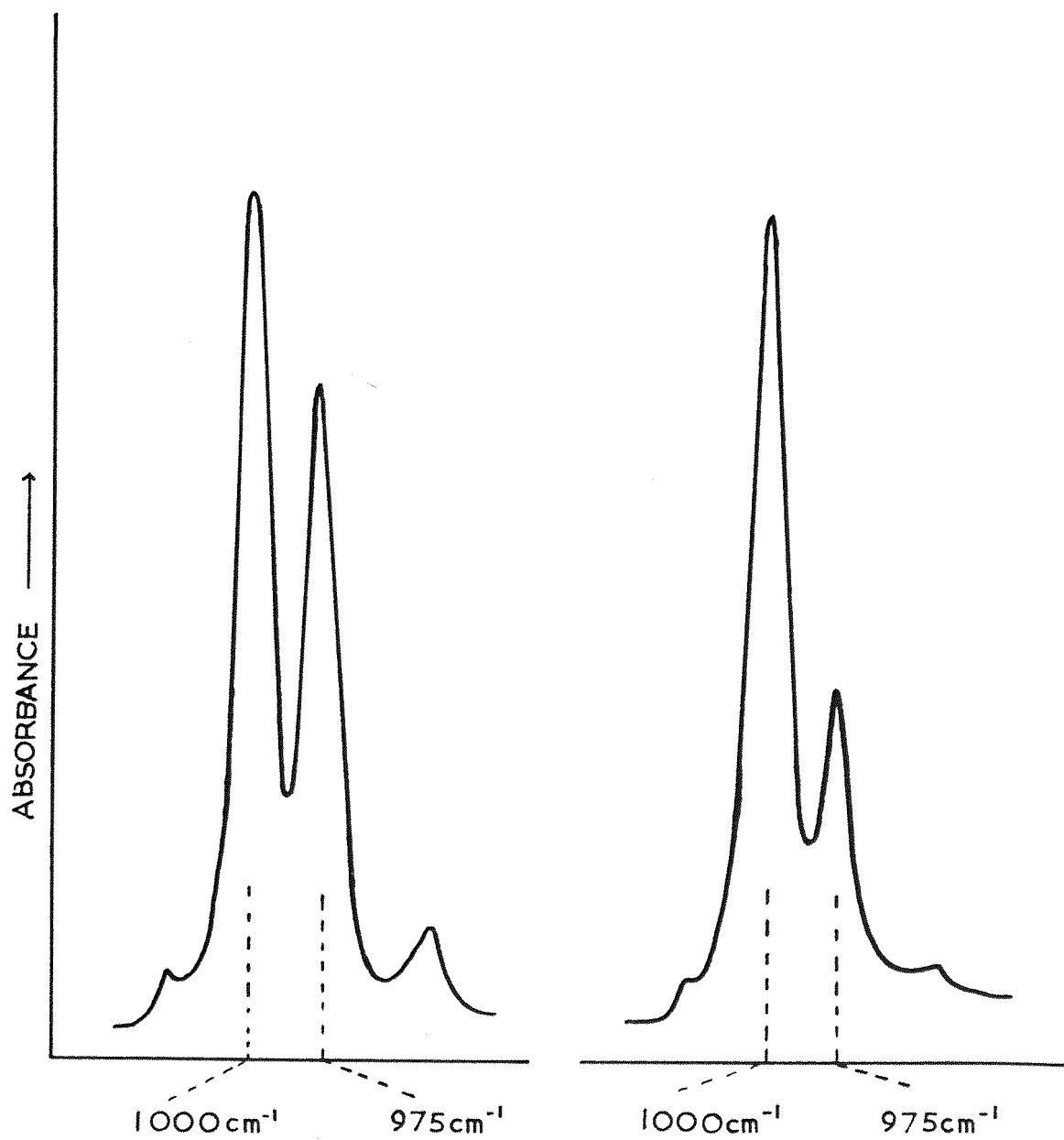


FIGURE 3.
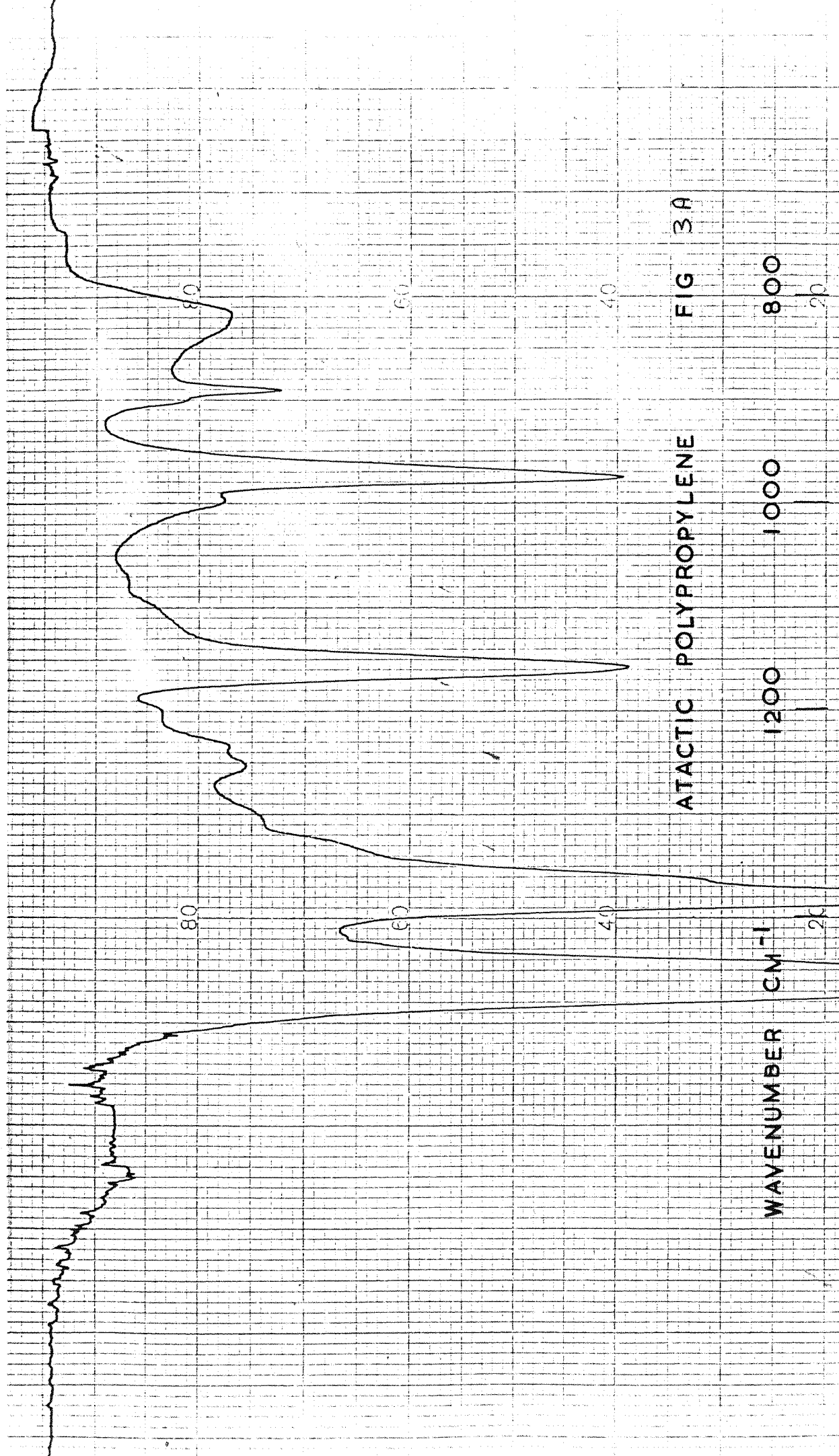
ATACTIC POLYPROPYLENE

WAVENUMBER CM⁻¹

FIG 3A
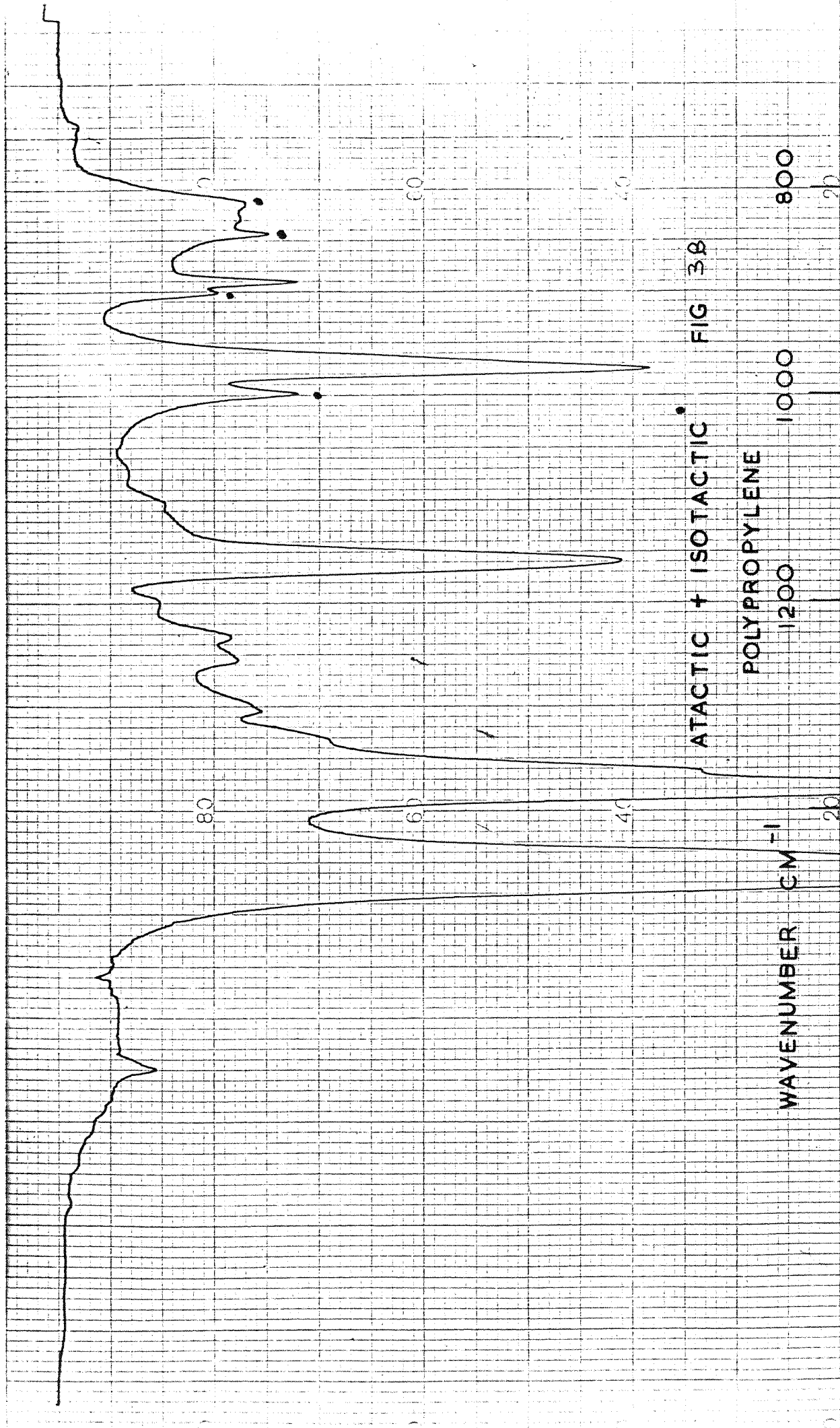
ATACTIC + ISOTACTIC

POLYPROPYLENE

FIG. 38

WAVENUMBER CM⁻¹
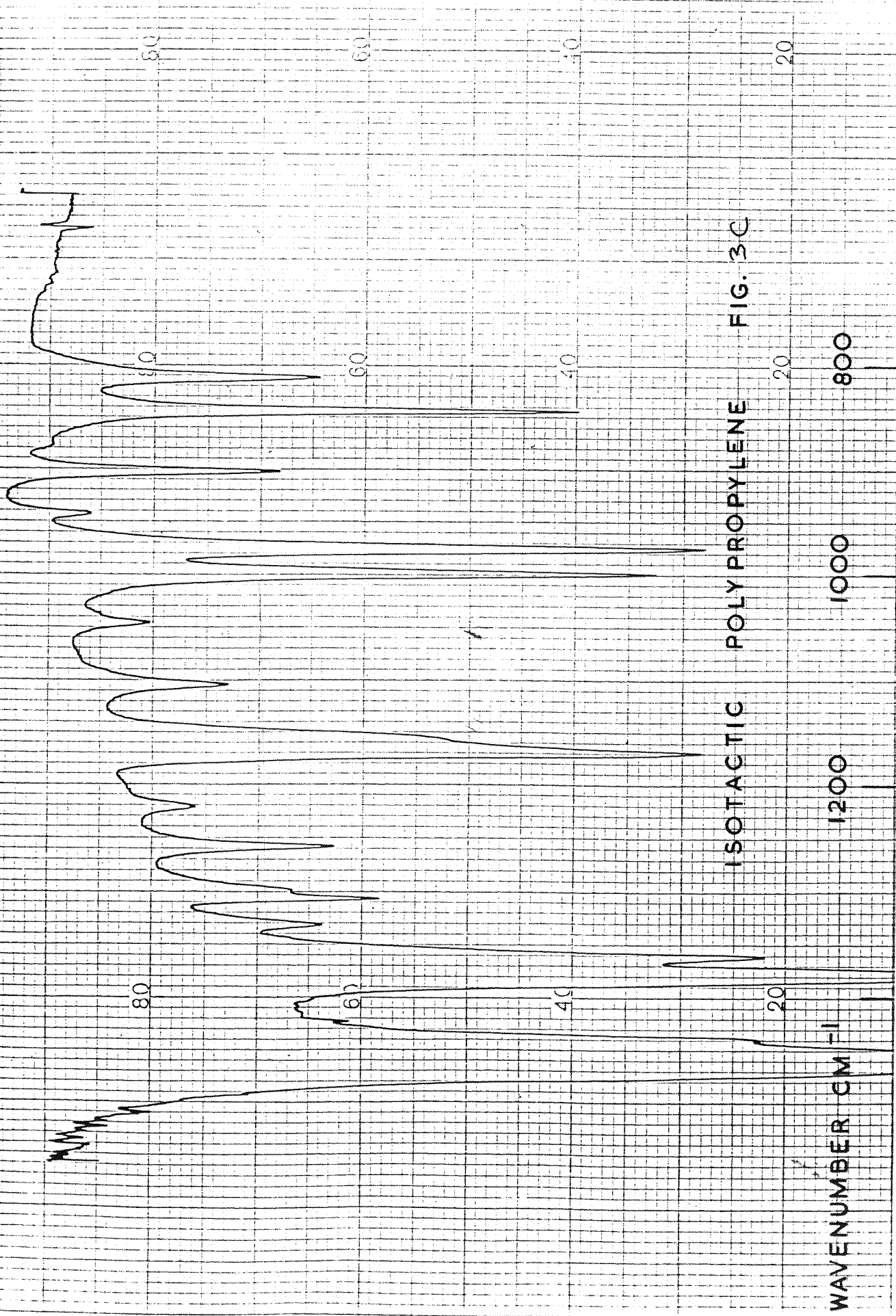
ISOTACTIC POLYPROPYLENE  FIG. 3C

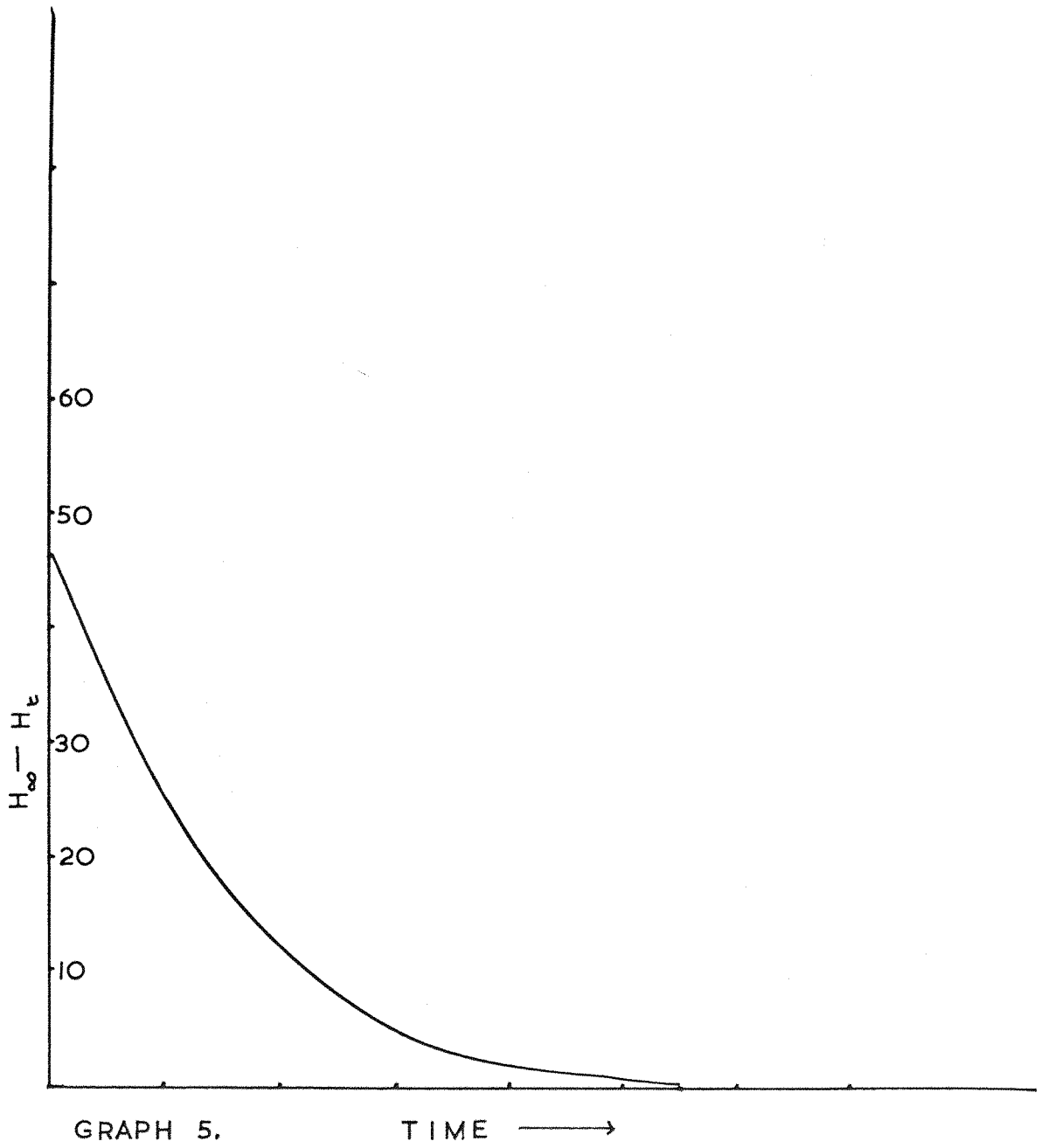WAVENUMBER CM⁻¹

TYPICAL  G P C    TRACE
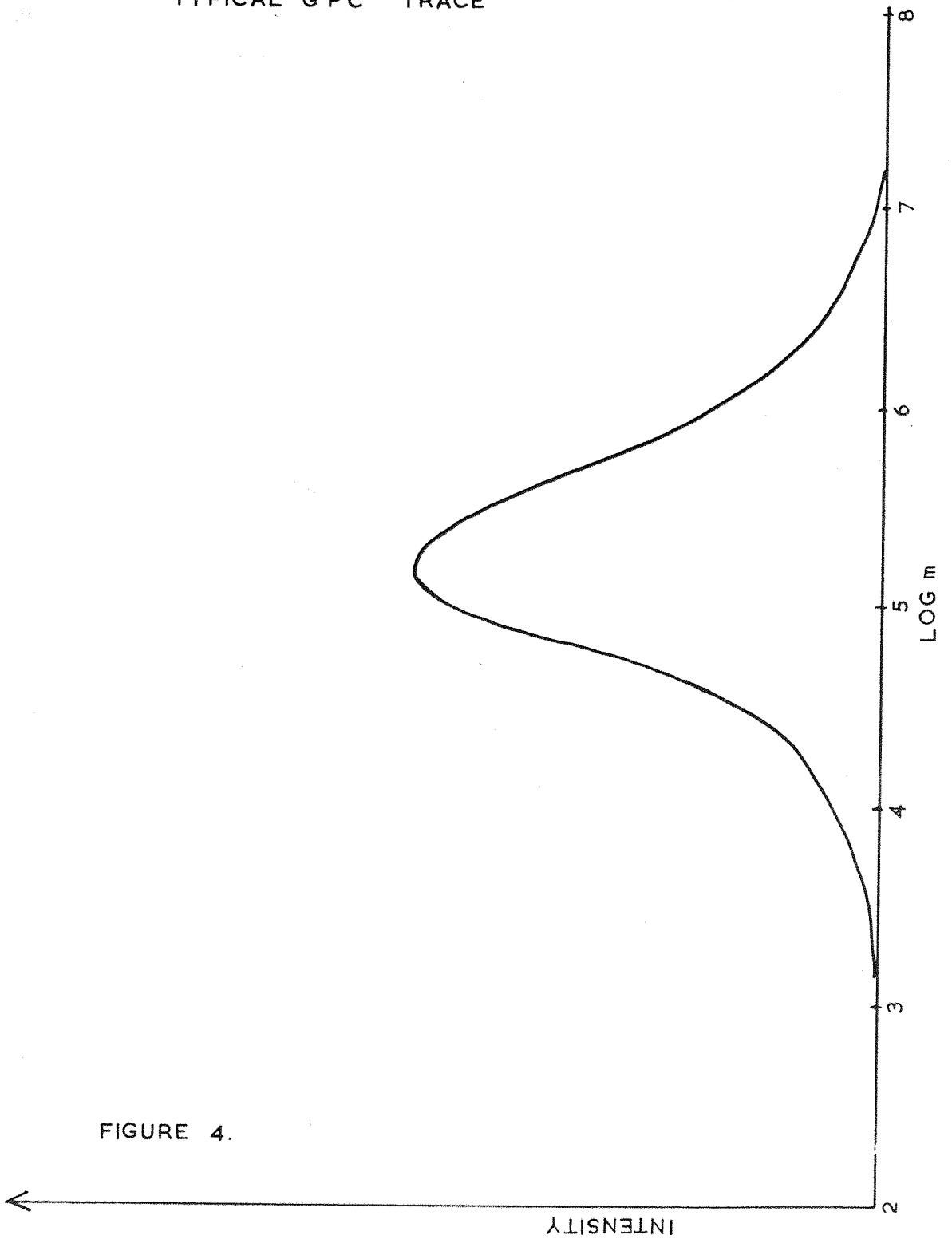


FIGURE  4.

WHOLE   POLYMERS   A , B , C.



GRAPH I.

HEPTANE INSOLUBLES SAMPLES A,B,C.

GRAPH 2.

HELICAL CONTENT %
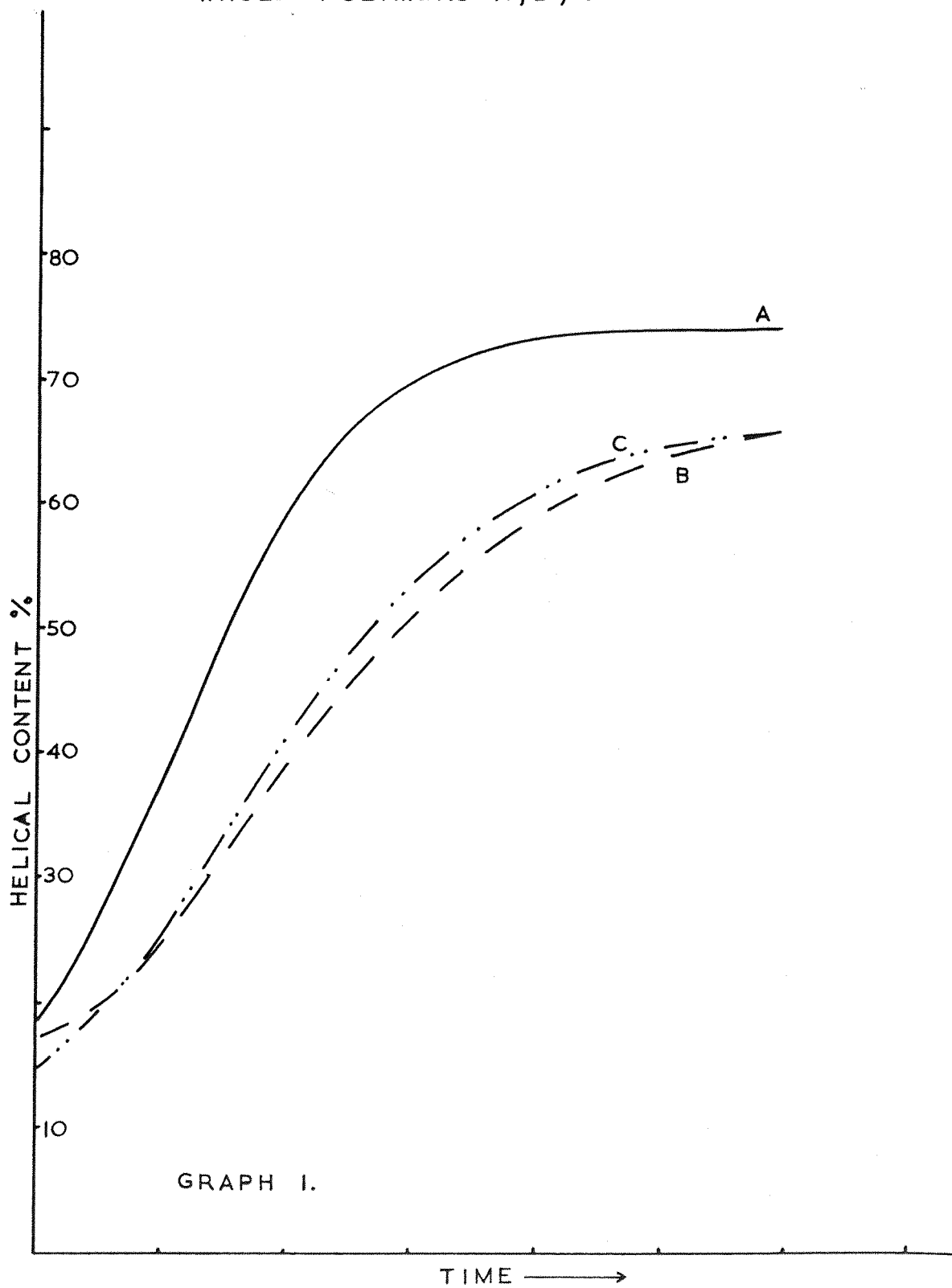
TIME
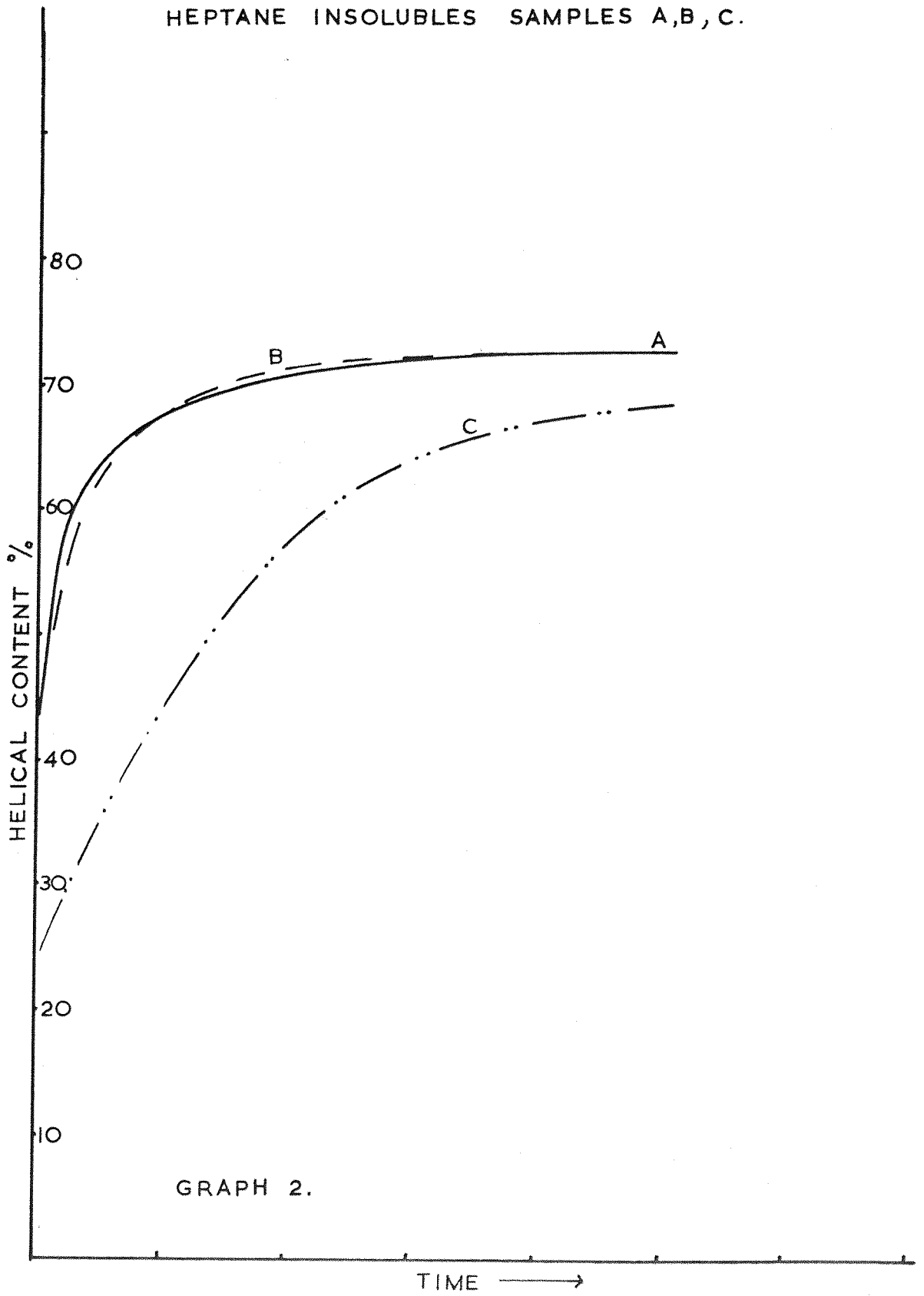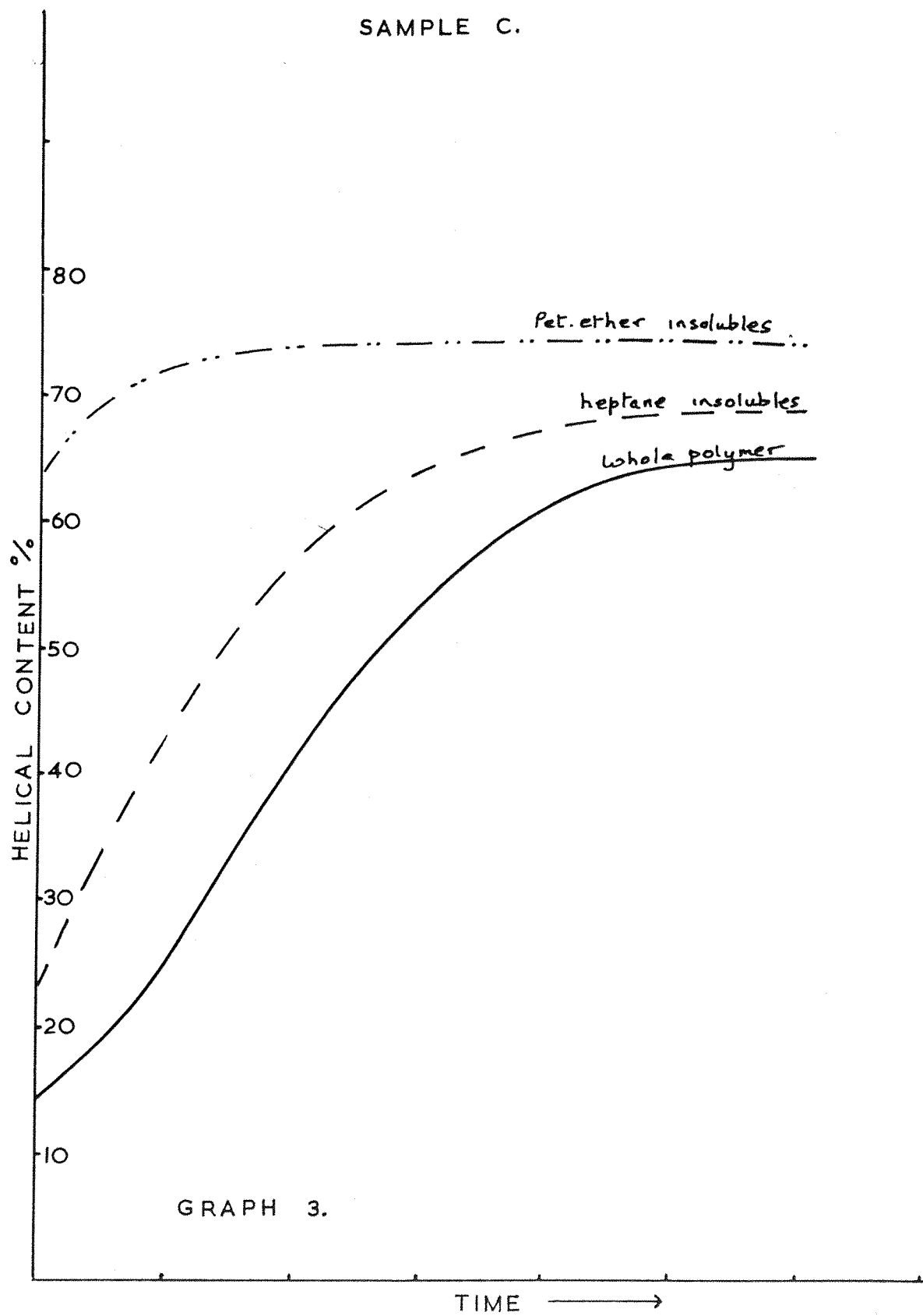
SAMPLE C.

GRAPH 3.

SAMPLE C   WHOLE   POLYMER
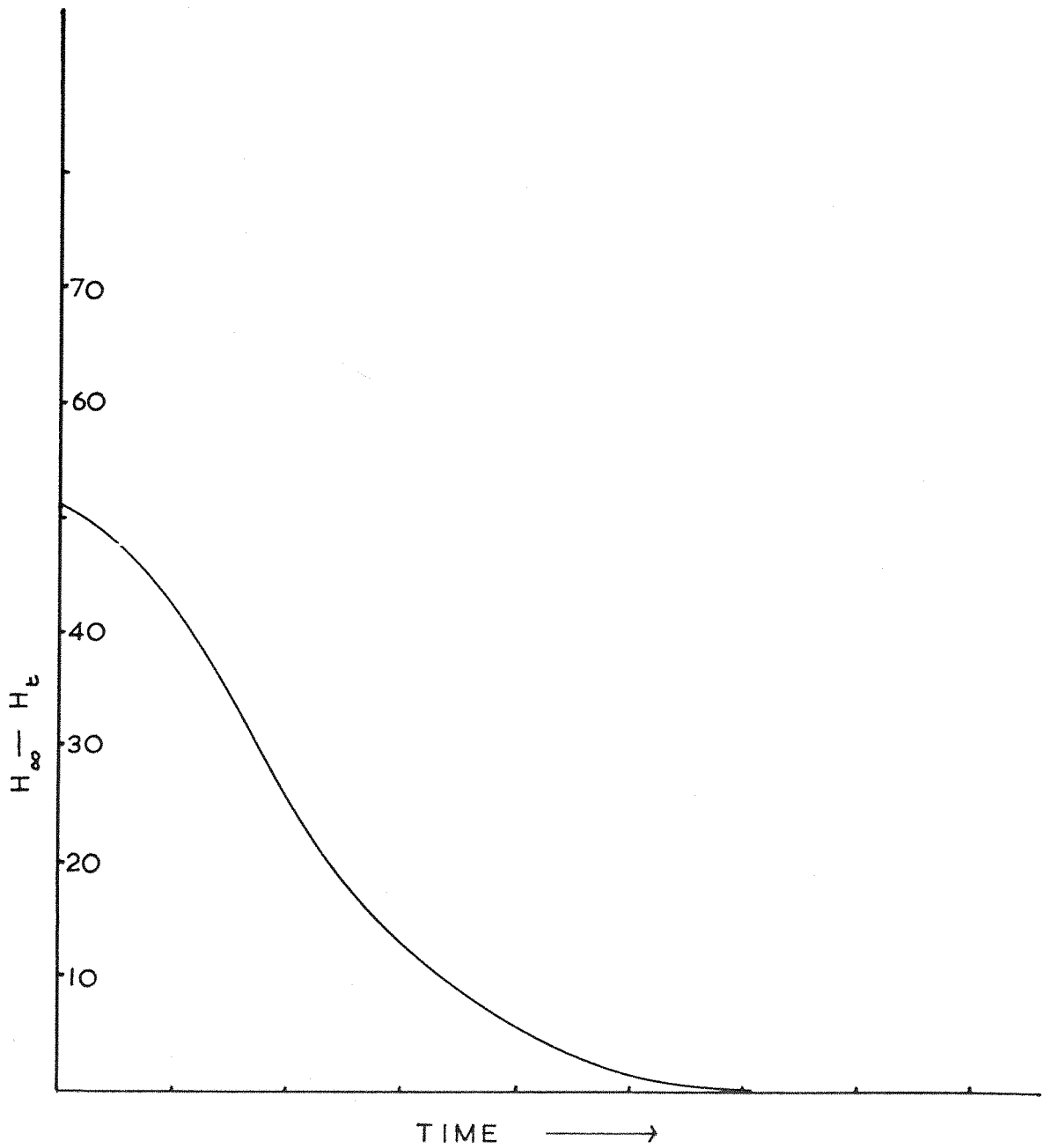


GRAPH  4.

SAMPLE C   HEPTANE INSOLUBLES



GRAPH 5.          TIME ⟶

SAMPLE C    PET. ETHER   INSOLUBLES
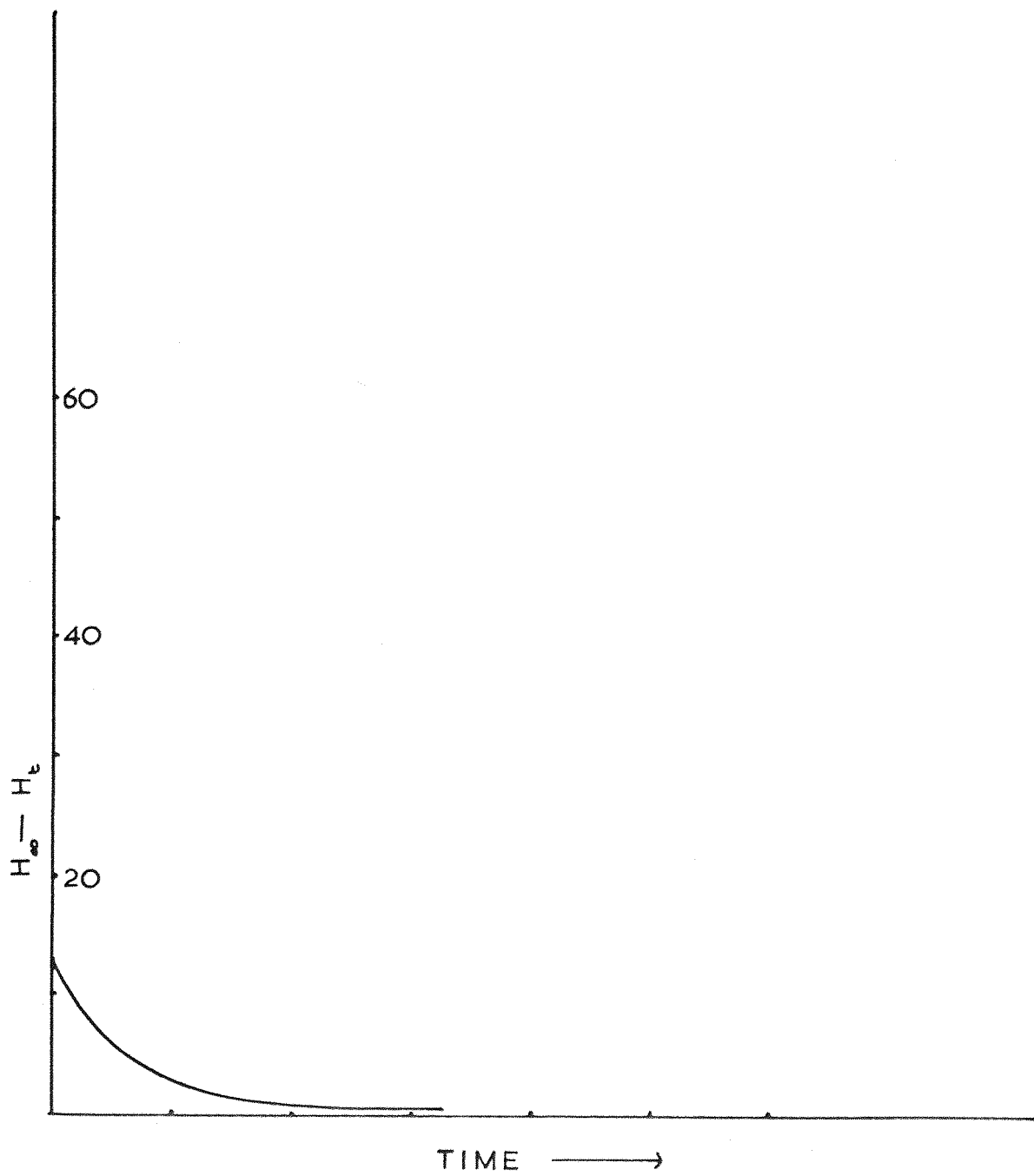
GRAPH 6.

SAMPLE   C    WHOLE   POLYMER
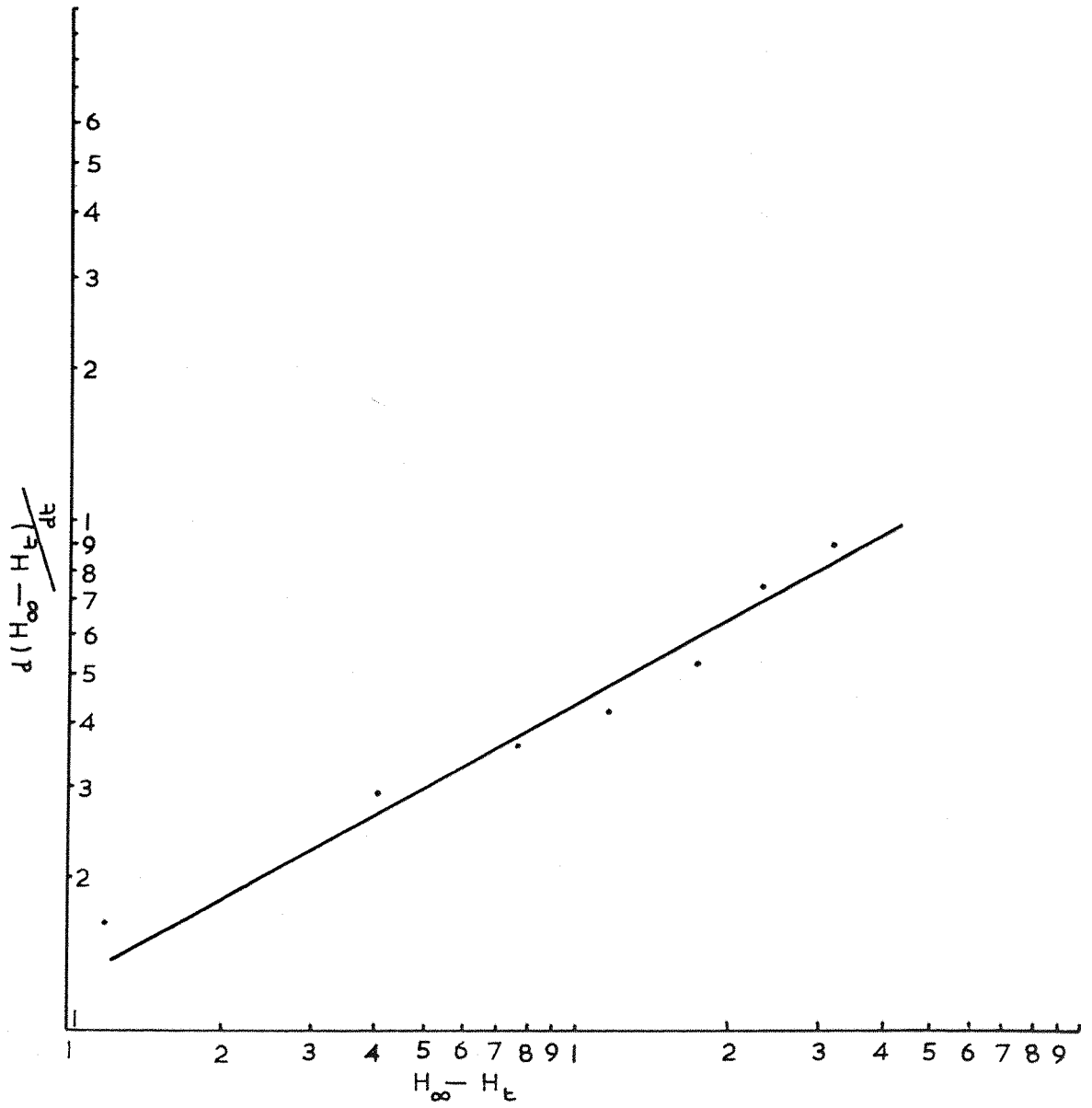


GRAPH   7.

SAMPLE C HEPTANE INSOLUBLES
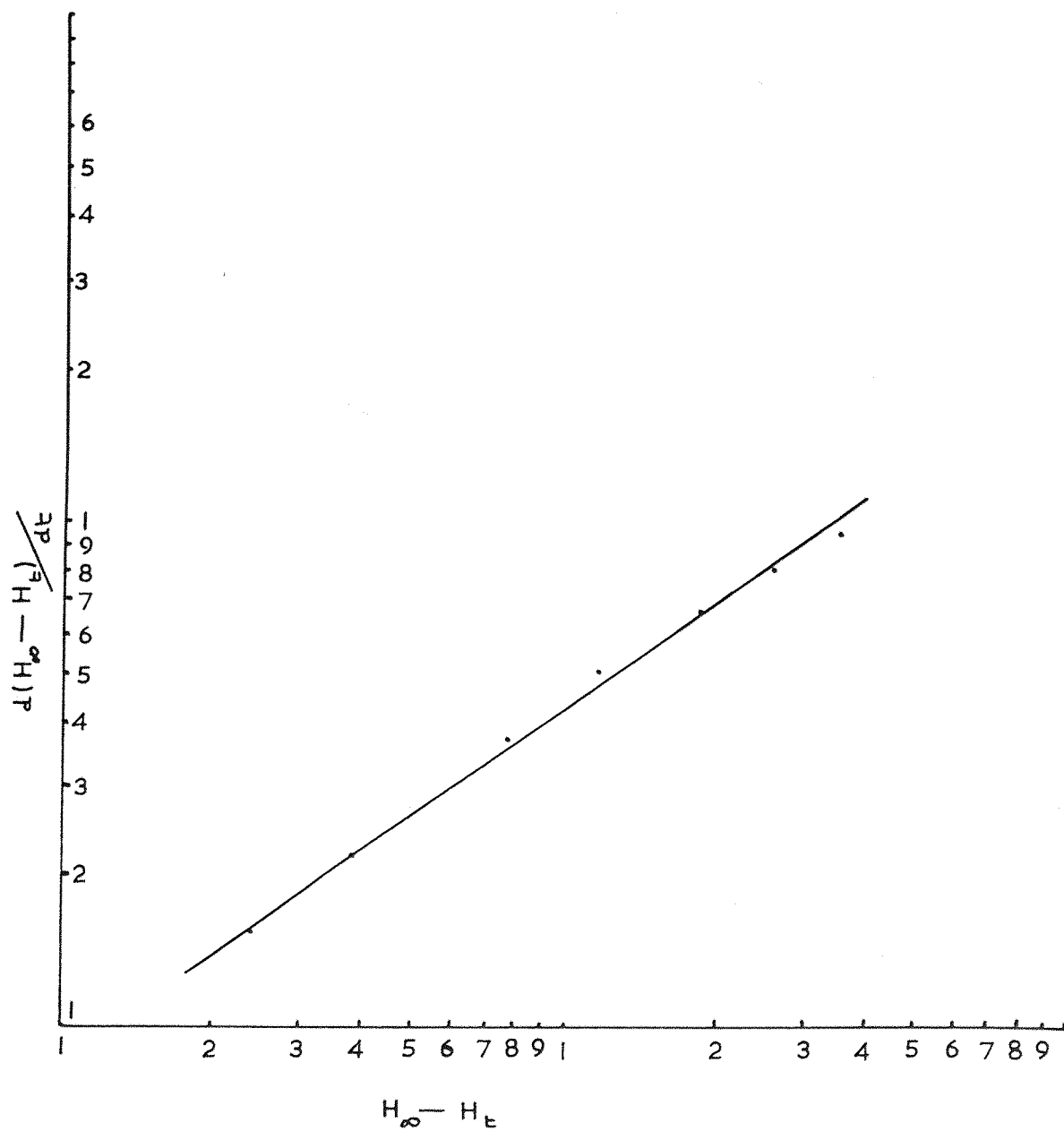


GRAPH 8.
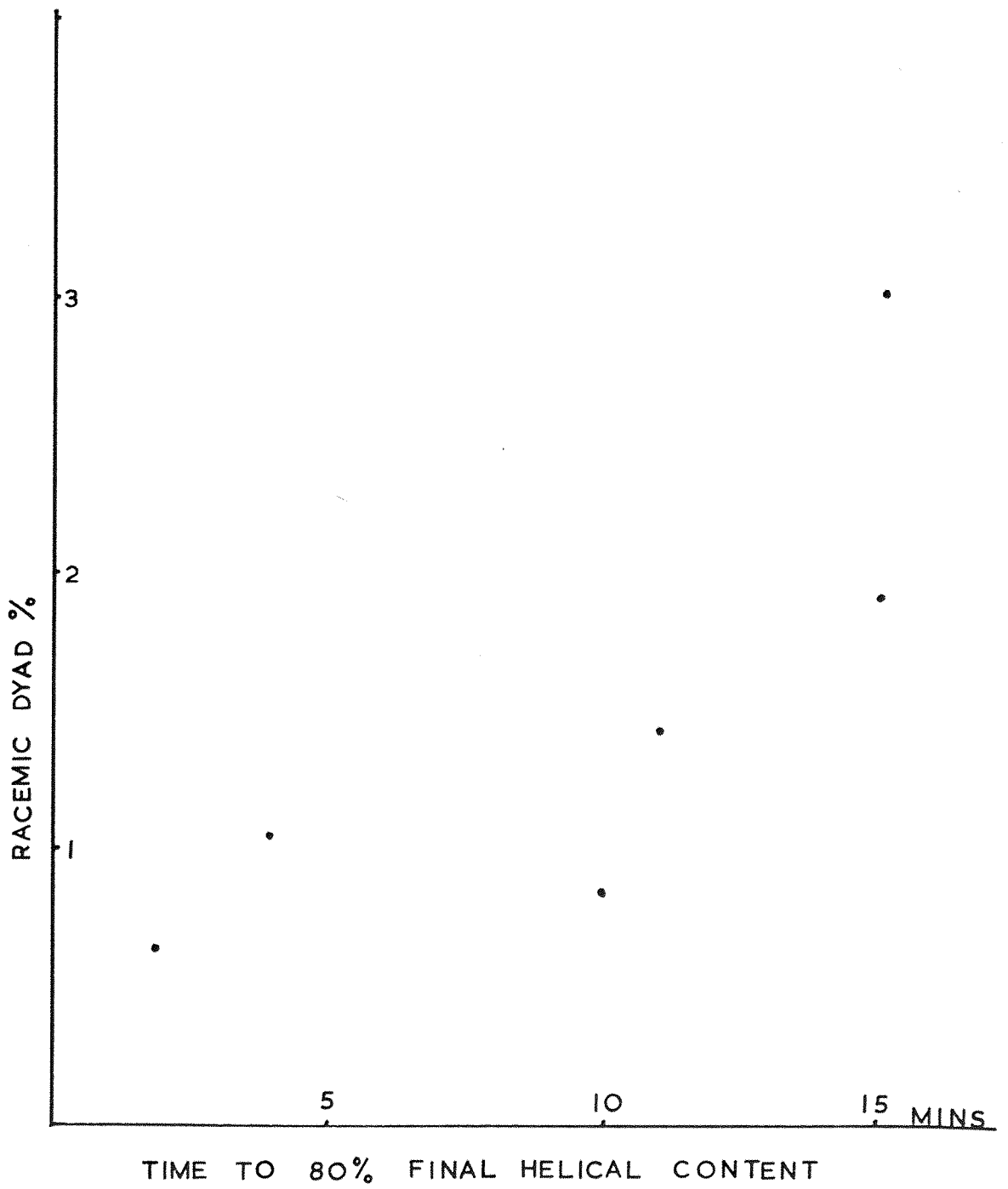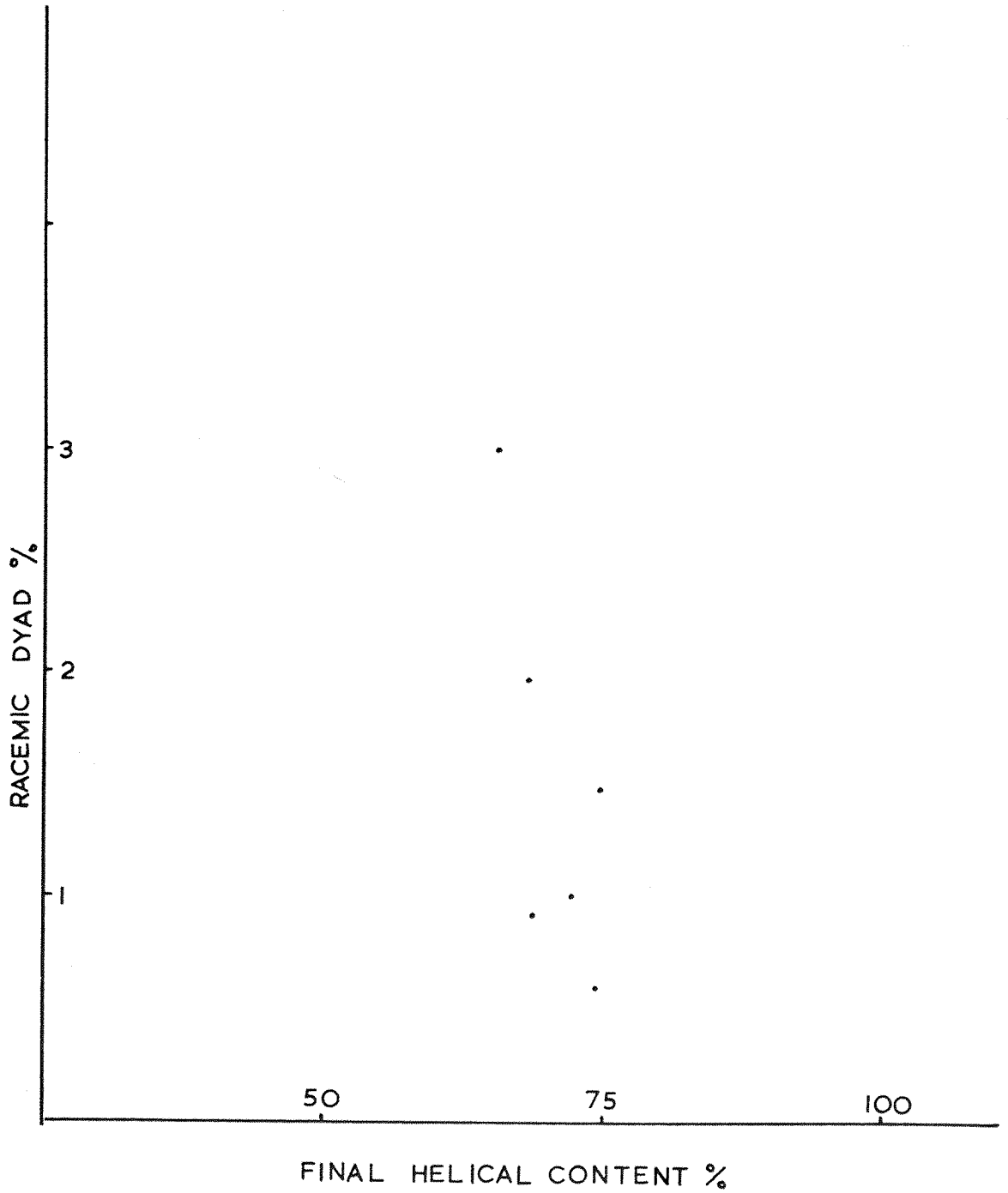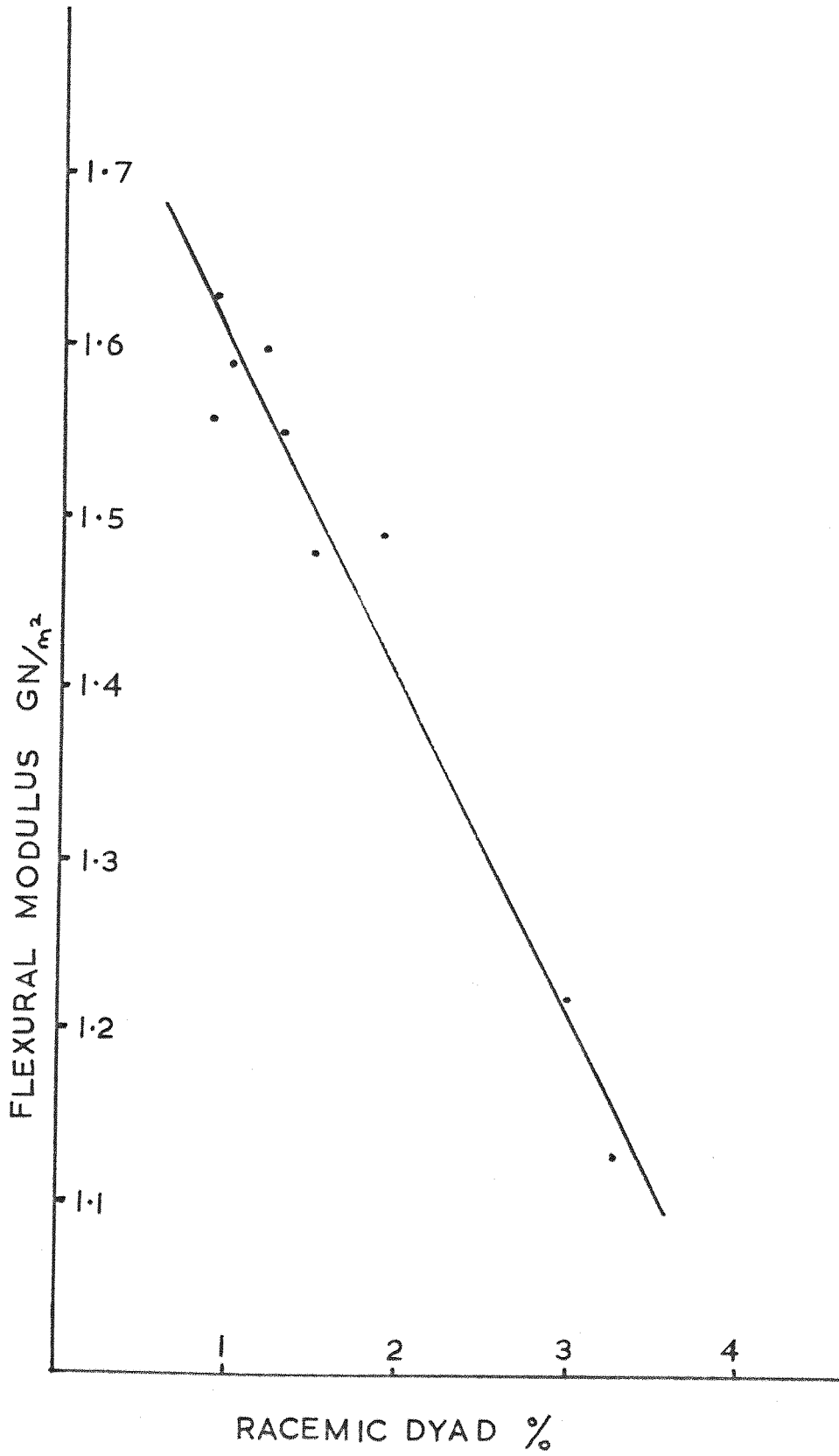
SAMPLE   C   PET. ETHER   INSOLUBLES
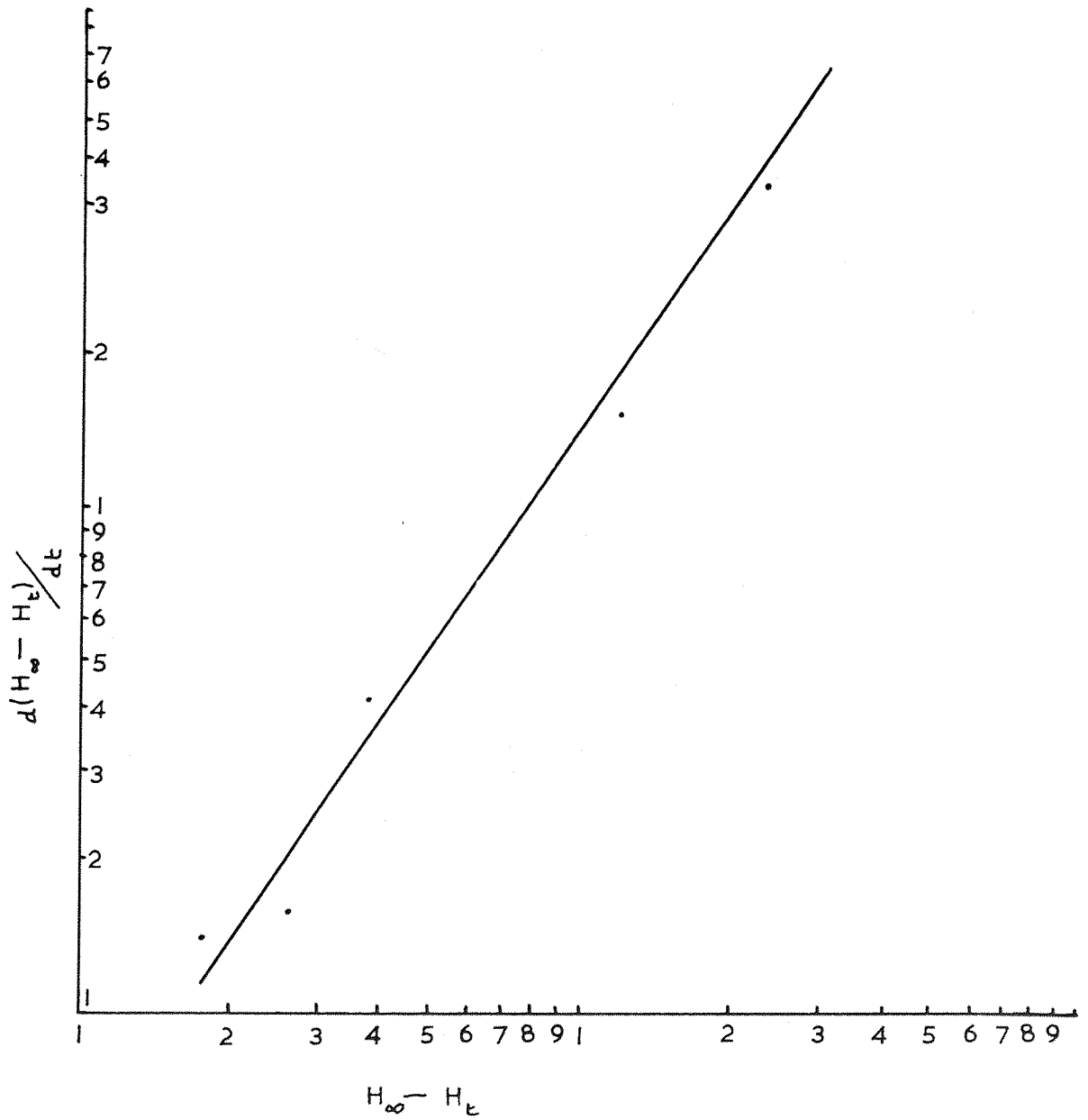


GRAPH  9.
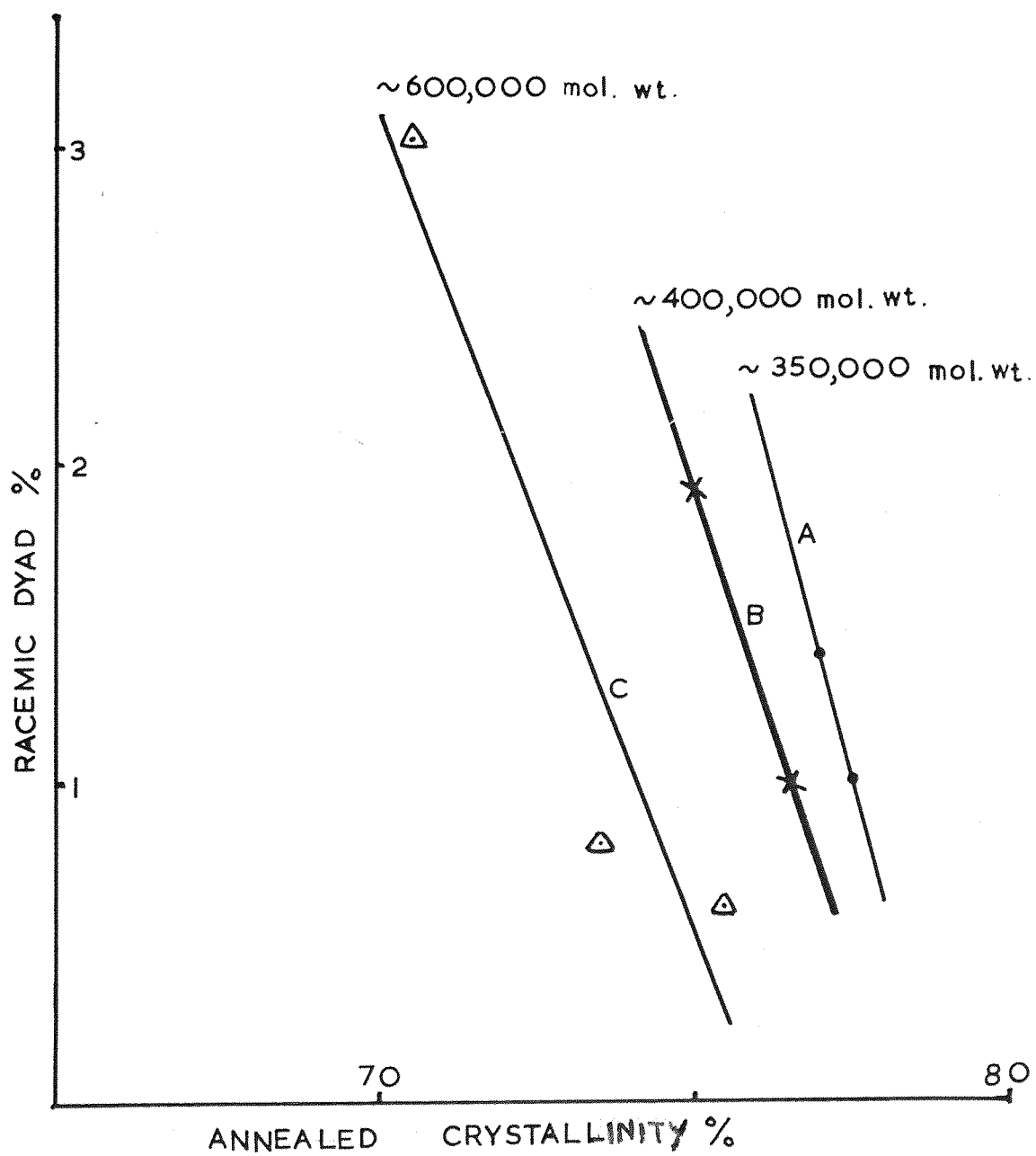
GRAPH 10.

GRAPH II.

GRAPH 12.

GRAPH 13.

# Solid-state High-resolution $^{13}$C N.m.r. Spectra of Polypropene

By Alan Bunn and Michael E. A. Cudby

(*ICI Plastics Division, Welwyn Garden City, Herts.*)

and Robin K. Harris,* Kenneth J. Packer,* and Barry J. Say

(*School of Chemical Sciences, University of East Anglia, Norwich NR4 7TJ, Norfolk*)

# Solid-state High-resolution $^{13}$C N.m.r. Spectra of Polypropene

By Alan Bunn and Michael E. A. Cudby

(*ICI Plastics Division, Welwyn Garden City, Herts.*)

and Robin K. Harris,* Kenneth J. Packer,* and Barry J. Say

(*School of Chemical Sciences, University of East Anglia, Norwich* NR4 7TJ, *Norfolk*)

*Summary* The high-resolution $^{13}$C n.m.r. spectra of solid isotactic and syndiotactic polypropene are reported and a novel confirmation of the specific helical nature of syndiotactic polypropene previously deduced from X-ray diffraction studies is given.

Schaefer and Stejskal[1] combined the heteronuclear polar-decoupling and cross-polarisation techniques[2] with magic-angle sample rotation[3] to demonstrate that $^{13}$C n.m.r. spectra of organic solids could be obtained with high resolution. In this communication we describe some preliminary results from isotactic and syndiotactic polypropene in the solid state. The spectra were obtained using a home-built spectrometer operating at 22·6 MHz for C with a magic-angle rotation speed of *ca.* 2·3 kHz.[4,5] The $^{13}$C n.m.r. spectrum of a solid rotor of the $\alpha$-form[6] of isotactic polypropene showed three resonance peaks assigned to methyl, methine, and methylene carbons (see Table). The chemical shifts differ from those found for the same polymer in the solution state where the molecules are thought to exist as random coils. In contrast, the crystalline regions of isotactic polypropene are known to be composed of regular arrays of helical molecules.[6] The unit cell contains four polymer molecules where each molecule is in the form of a helix having three monomer units per complete turn. X-Ray studies showed that the polypropene used in this work was approximately 75% crystalline. However, the total helical content was shown[7] by i.r.

spectroscopy to be *ca.* 85%. We believe that the solid-state chemical shifts found for isotactic polypropene are largely dependent on intramolecular effects. Thus, the helical nature of the polymer is more important than the packing of the helices in the crystalline regions in determining the chemical-shift values observed. However, as noted elsewhere,[5] the widths of the resonance lines from the different carbons in isotactic polypropene are not the same. In addition, determination of the spectrum by a pulse sequence in which the $^{13}$C contact pulse is delayed by various amounts following the spin-locking of the protons produces considerable changes in these line shapes, even resulting in splittings for certain other, related, polymers. We believe that these observations relate to the fact that a polymer such as isotactic polypropene contains amorphous regions, and that finer details of the crystal structure may lead to structure on the individual resonances from the crystalline region. Future publications will amplify these observations and deal with polyolefins in general.

Figure 1 shows the $^{13}$C n.m.r. spectrum of solid syndiotactic polypropene in powder form, packed into a hollow glass rotor.[5] Solution-state $^{1}$H n.m.r. spectroscopy at 220 MHz showed the material to be highly syndiotactic ($>$ 95% racemic dyads). The chemical shifts observed for resonances in the solid-state spectrum are significantly different from those obtained in the solution state (see Table) but by far the most important difference between the spectra taken in the two states is the doubling of the methy-

Table. The $^{13}$C chemical shifts of isotactic and syndiotactic polypropenes in solution and solid states.

| | $\delta_C$/p.p.m. | | | | | |
|---|---|---|---|---|---|---|
| | Methyl | | Methylene | | Methine | |
| Material | Solution[a] | Solid | Solution[a] | Solid | Solution[a] | Solid |
| Isotactic | 21·58 | 22·5 | 45·54 | 44·5 | 27·86 | 26·5 |
| Syndiotactic | 19·90 | 21·0 | 46·14 | 39·6 and 48·3 | 27·45 | 26·8 |

Since the chemical shifts of polypropene are temperature-dependent,[12] the values quoted are obtained from atactic polypropene, which is soluble in *o*-dichlorobenzene at room temperature, in contrast to the other forms which require considerably elevated temperature to form a solution.
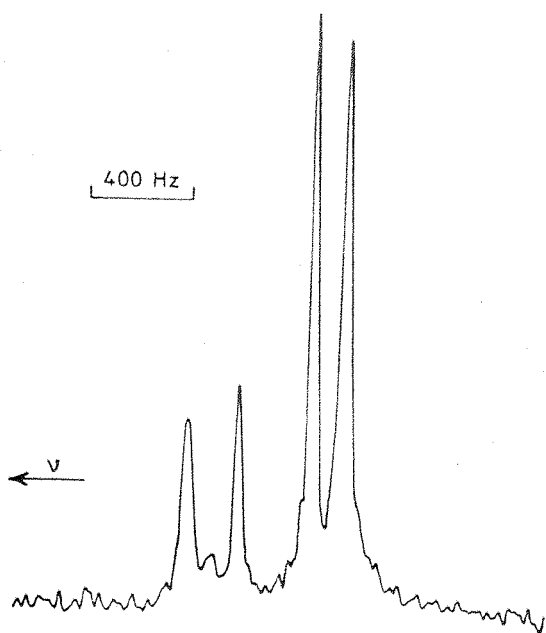
400 Hz

← ν

IGURE 1. The $^{13}$C n.m.r. spectrum of ca. 70 mg of powdered yndiotactic polypropene at ca. 300 K. The spectrum was btained by co-adding $5 \times 10^4$ free-induction decays generated y cross-polarisation using a single contact pulse of 1 ms per ꓹ spin-locking and a recycle time of 1 s. Magic-angle rotation t ca. 2·3 kHz was employed.
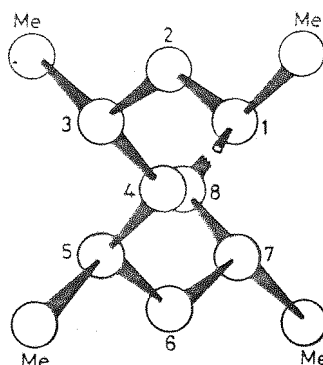


FIGURE 2. A view of the conformation of syndiotactic polypropene, according to Corradini et al.,[10] looking down the helix axis. The backbone methine and methylene carbons are numbered sequentially for clarity with the methyl carbons labelled Me. The two non-equivalent sites for the methylene carbons are clear, being typified by atoms 2 and 6, and 4 and 8 respectively.

ne carbon resonance in the solid-state spectrum. The ꓲagnitude of the chemical-shift difference between the two ꓲethylene peaks is a larger effect than has been reported ꓲr any other polymer system.[8,9] We suggest that the ꓲason for the two methylene resonances in the solid-state ꓲectrum of syndiotactic polypropene lies in the conformaꓲon of the polymer molecule in the solid. Corradini et al. ꓲggested from X-ray diffraction studies that the conformaꓲon of syndiotactic polypropene is an involuted helix ꓲaving the appearance of a figure-of-eight when viewed ꓲwn the helix axis[10] (Figure 2). Examination of this ꓲructure shows that there are two equally probable, distinct, ꓲtes for methylene carbons, one lying on the axis of the ꓲꓲlix (numbers 4 and 8 in Figure 2), the other on the periꓲꓲery of the helix (2 and 6 in Figure 2), whereas there are ꓲꓲly single sites for methine and methyl carbons. The ꓲꓲmber of peaks in the spectrum is therefore consistent with ꓲꓲs structure. The chemical-shift difference of $8·7 \pm 0·5$ p.m. observed between the two methylene-carbon ꓲsonances is considered to arise largely from 3-bond interꓲꓲtions (the γ-effect).[11] The internal methylene carbons ꓲ and 8 in Figure 2) have two gauche γ-carbons, whereas the ꓲter methylenes (2 and 6 in Figure 2) have two trans γ-

carbons. Recently published data[12] indicate that the γ-gauche shielding effect in polypropene is ca. 4 p.p.m. Our measurements give a value of 4·4 p.p.m. for this effect, assuming it to be the dominant cause of the observed splitting. If the γ-effect is the cause of the difference in the chemical shift of the two methylene resonances then the resonance at $\delta_C = 39·6$ p.p.m. is assigned to the internal methylene carbons (4 and 8 in Figure 2). In support of this, the other methylene resonance at 48·3 p.p.m. is broader than that at 39·6 p.p.m., and shows evidence of asymmetry and even splitting under higher scale-expansion. As noted above we believe that such effects may arise from details of the solid-state structure related, at least in part, to interchain effects and it would be reasonable that those atoms on the periphery of the helical chain would be more subject to such perturbations.

We feel that the major features of these spectra are explicable in terms of the known structures and γ-shielding effects, and it should be noted that, on such a basis, the resonance arising from the methylene carbon in α-isotactic polypropene should occur at a chemical shift midway between those for the two different methylenes of the syndiotactic form. This is indeed the case and confirms that the main effects determining the chemical shifts are intramolecular in origin. The question of the finer structure of the resonance lines will be pursued in more detail elsewhere.

[1] J. Schaefer and E. O. Stejskal, J. Am. Chem. Soc., 1976, 98, 1031.
[2] A. Pines, M. G. Gibby, and J. S. Waugh, J. Chem. Phys., 1973, 59, 569.
[3] E. R. Andrew, Prog. Nucl. Magn. Reson. Spectrosc., 1971, 8, 1.
[4] R. K. Harris, K. J. Packer, A. G. Oliver, and B. J. Say, Proc. European Conference on N.m.r. of Macromolecules, Sardinia, May
   —11, 1978, p. 29.
[5] G. Balimann, M. J. S. Burgess, R. K. Harris, A. G. Oliver, K. J. Packer, B. J. Say, S. F. Tanner, R. W. Blackwell, L. W. Brown,
   Bunn, M. E. A. Cudby, and J. W. Eldridge, J. Chem. Phys., 1980, 46, 469.
[6] A. Turner-Jones, J. M. Aizlewood, and D. R. Beckett, Makromol. Chem., 1964, 75, 134.
[7] M. Fujiyama, H. Awaya, and K. Aguma, J. Polym. Sci., Polym. Lett. Ed., 1980, 18, 105.
[8] J. Schaefer, E. O. Stejskal, and R. Buchdahl, Macromolecules, 1977, 10, 384.
[9] G. A. Gray and H. D. W. Hill, Ind. Res. Dev., 1980, 22, 136.
[10] P. Corradini, G. Natta, P. Ganis, and P. A. Temussi, J. Polym. Sci., 1967, C16, 2477.
[11] D. M. Grant and E. G. Paul, J. Am. Chem. Soc., 1964, 86, 2984.
[12] F. C. Schilling and A. E. Tonelli, Macromolecules, 1980, 13, 270.

# High resolution $^{13}$C n.m.r. spectra of solid isotactic polypropylene

## A. Bunn and M. E. A. Cudby
*ICI Petrochemicals and Plastics Division, Welwyn Garden City, Hertfordshire, UK*

## and R. K. Harris, K. J. Packer and B. J. Say
*School of Chemical Sciences, University of East Anglia, Norwich, NR4 7TJ, Norfolk, UK*
*(Received 17 June 1981; revised 7 October 1981)*

The high-resolution $^{13}$C n.m.r. spectra of three samples of solid isotactic polypropylene are reported. The spectra, obtained under conditions of proton dipolar-decoupling and fast magic-angle rotation and using cross-polarization, are of annealed and quenched samples of the α-crystalline form and of a sample of the β-crystalline form. Attention is drawn to the importance of knowing the proton relaxation characteristics in these experiments and some illustrative proton $T_{1\rho}$ data are given. The $^{13}$C n.m.r. spectrum of the annealed sample of the α-crystalline form shows well-resolved splittings of the methyl and methylene resonances in a 2:1 intensity ratio. These splittings are interpreted in terms of the crystal structure of the α-form as suggested by X-ray diffraction. Quenching the α-form causes significant changes in the spectrum including a loss of resolution of the splittings obtained from the annealed sample. The β-form shows broad symmetrical resonances for the methyl and methylene carbons. The chemical shifts and other spectral features are discussed in the light of the proposed crystal structures and the effects likely to be produced by quenching.

**Keywords** Solids; polymers; polypropylene; structure; polymorphism; nuclear magnetic resonance

## INTRODUCTION

In a previous communication concerning the high-resolution $^{13}$C n.m.r. spectroscopy of solid polypropylene[1] it was indicated that a more detailed examination of the spectra of the solid isotactic form was in progress. This paper reports the results of this further investigation and concerns the dependence of the solid-state spectra on the history of the physical treatment of the sample and the relationship of these spectra to the structure of the crystalline regions of the materials.
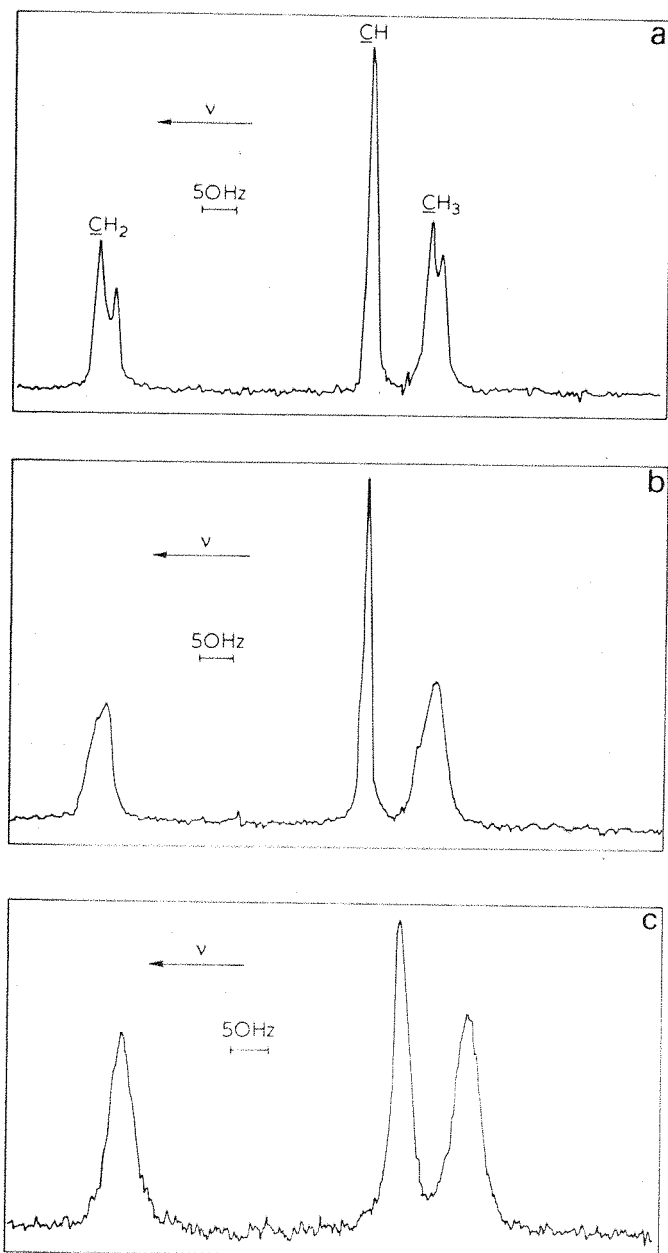
## EXPERIMENTAL

### N.m.r. measurements

The high-resolution $^{13}$C spectra were obtained using a purpose-built spectrometer which operates at 22.63 MHz for $^{13}$C (90 MHz, $^{1}$H). The usual spin-locked cross-polarization method was used for generating the $^{13}$C signals[2]. Cross-polarization was generally carried out with r.f. field strengths of 40 kHz whilst the proton-dipolar decoupling field strength used was 60 kHz. Magic-angle sample rotation speeds of the order of 2 kHz were employed and were achieved using the device described elsewhere[3]. Some of the spectra reported here contain features whose chemical shift differences are of the order of 0.5 ppm and in order to observe such features reproducibly, it was found necessary to use decoupling fields of at least 60 kHz and to pay careful attention to setting the magic-angle and to shimming of the static field. To this end a rotor filled with water and spinning slowly at the magic-angle was used to adjust the field inhomogeneity. It is of some interest to note that the normal high-resolution shim coils used in electromagnets and defined on the assumption of y-axis spinning[4] are not entirely satisfactory for samples rotating in the xz plane at the magic angle.

The spectrometer frequencies were calibrated regularly using a static sample of liquid tetramethylsilane as a reference for both $^{1}$H and $^{13}$C. It is clearly impossible to avoid the problems of bulk-susceptibility shifts in the study of n.m.r. of solids as the use of external chemical shift references is the only means of calibration. For the samples investigated in this paper these effects are likely to be small as they were all the same chemical species and were all examined as rolled thin films in identical rotors. However, in general, care must be taken in making comparisons of chemical shifts from one sample to another.

In order to optimize the experimental conditions used in obtaining the $^{13}$C spectra *via* cross-polarization it is our normal practice to determine the proton spin-lattice relaxation times in both laboratory and rotating frames. A detailed study of these relaxation processes for the polypropylene samples used in the work is under way but certain features are relevant to the interpretation of the $^{13}$C spectra and so details of these measurements follow. These relaxation processes have been measured at a proton resonance frequency of 60 MHz using a home-built pulsed n.m.r. spectrometer. $T_1$ was measured using the 180–τ–90 pulse sequence whilst the $T_{1\rho}$ behaviour was investigated using the spin-locking sequence[5]. A spin-locking field strength of 1 mT (10 gauss ≡ 40 kHz) was used which is the same as the r.f. field strength used for the cross-polarization experiments. Since the $^{1}$H $T_{1\rho}$

*Figure 1*  $^{13}$C high-resolution n.m.r. spectra of various forms of solid isotactic polypropylene. The spectra were obtained as described in the experimental section with a cross-polarization contact time of 5 ms, a recycle time of 3 s and are the result of 4000 transients recorded with quadrature detection, a dwell time of 500 $\mu$s, an acquisition time of 256 ms and a filter bandwidth of 500 Hz. (a) The annealed $\alpha$-form; (b) the quenched $\alpha$-form and (c) the $\beta$-form

behaviour in these materials is dominated by low-frequency motions, the difference in spectrometer operating frequency for the relaxation and cross-polarization measurements (60 MHz and 90 MHz respectively) is unlikely to be significant.

*Sample preparation*

The polymer used in this investigation was a commercially available grade of polypropylene, manufactured by ICI Ltd., having a melt-flow index of 20. It had an isotactic content in excess of 97% as determined by proton magnetic resonance in solution from the racemic diad concentration[6]. For all samples the polymer was initially fabricated as a thin film in order to facilitate

rapid quenching and other procedures required to prepare the desired samples.

Three samples were prepared as follows: (i) an annealed sample of the $\alpha$ form, obtained by maintaining the film at a temperature of 433K for 60 min; (ii) a quenched sample of the $\alpha$ form obtained by rapidly cooling from the melt (at a temperature higher than 503K) by immersion in ice/water followed by rapid reheating to 373K and subsequent cooling to ambient temperature to remove any of the smectic form, and (iii) a sample of the $\beta$ form, obtained by rapid cooling from a melt temperature between 463K and 503K to a temperature between 373K and 393K. The final samples, in the form of thin films, were rolled into tight cylindrical rolls and inserted into 5 mm o.d. glass or machined Macor rotors. Typical sample weights were of the order of 50 mg. All measurements were made at ambient probe temperature.

RESULTS AND DISCUSSION

*Figure 1* shows the $^{13}$C n.m.r. spectra of the three samples investigated and gives the exact experimental conditions under which they were obtained. The major features of these spectra which are of note are (i) the observation for the annealed $\alpha$ form of well-resolved splittings of the resonance absorptions in the spectral regions associated with the methyl and methylene carbons; (ii) the reduced resolution of such splittings and the change in the intensity distributions in these regions for the quenched $\alpha$ form; (iii) the symmetrical lineshapes for these resonance absorptions in the $\beta$ form, and (iv) the relative chemical shifts of solution and solid samples.

*Table 1* summarizes the chemical shifts of the main peaks in the solid and solution state spectra.

Before discussing the features outlined above, it is worth considering the influence the experimental techniques used may have on the spectra. Of particular importance is the fact that many polymers are heterogeneous[7]. In the case of polypropylene, for example it is generally accepted that it consists structurally of organized or crystalline regions separated by regions which are less dense and less organized, usually referred to as amorphous. The relative dimensions of these regions may be altered by various physical treatments. From the point of view of $^{13}$C n.m.r. spectra, in which the signal is generated by polarization transfer from protons, this structural heterogeneity may have a significant effect. For example, the proton magnetic resonance spectrum of the annealed sample of $\alpha$-isotactic polypropylene at room temperature consists of a broad line, which accounts for the major part of the intensity, and a narrow line which is no more than 10% of the intensity. Investigation of the relaxation of the spin-locked proton magnetization of this sample revealed a decay which required a minimum of

*Table 1* The observed $^{13}$C chemical shifts (ppm from external TMS; relative shifts accurate to ±0.1 ppm) of the principal features in the n.m.r. spectra of various solid samples of polypropylene

| Sample | CH$_2$ | CH | CH$_3$ |
|---|---|---|---|
| $\alpha$-Crystalline | 45.2  44.2 | 26.8 | 22.6  22.1 |
| $\alpha$-Quenched | 44.2 | 26.8 | 22.1 |
| $\beta$-Crystalline | 45.0 | 27.1 | 22.9 |
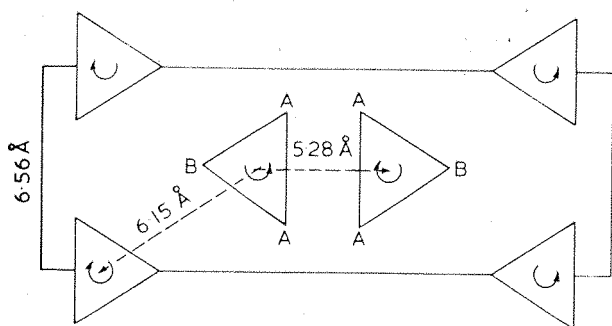
**Figure 2** Structure of the α-form of solid isotactic polypropylene as determined by X-ray diffraction[8,9]. The figure shows a projection perpendicular to the molecular axis. The triangles represent the isotactic polypropylene molecules which have a 3 : 1 helical conformation. The arrows represent the handedness of each helix. The labels A and B identify the inequivalent sites discussed in the text which, because the CH−CH₂ bond is almost parallel with the *c*-axis[8], are applicable to all three types of carbon site, i.e. methyl, methine and methylene. It should be noted that the structure consists of paired helices of opposite handedness with their centre-to-centre separation of 5.28 Å substantially less than the separation from other helices

three exponential processes for its description. Treated as a three-component decay, the relative intensities and relaxation times were 48% with $T_{1\rho} = 108$ ms; 25% with $T_{1\rho} = 15$ ms and 27% with $T_{1\rho} = 0.83$ ms. In addition it was shown that the narrow line in the spectrum was associated with the fastest $T_{1\rho}$ process, although clearly not accounting for all of it. The proton spin-lattice relaxation, however, was found to be indistinguishable from a single exponential process ($T_1 \simeq 700$ ms). These observations are consistent with a heterogeneous structure which, in its simplest form, can be considered to have three different environments in which the molecular motions, and, hence, relaxation times, differ. These different environments must have dimensions which are in the right range to allow spin-diffusion to average the $T_1$'s but not the (shorter) $T_{1\rho}$ values[7]. This type of behaviour is well recognized but its implications for cross-polarization have not been given much attention. In the case of the annealed sample we find that to a good approximation we are only generating [13]C n.m.r. signal intensity from those carbons associated with the two longer proton $T_{1\rho}$'s and the broader parts of the proton spectrum. This is almost certainly some fraction of the more crystalline part of the material since efficient cross-polarization requires a strong, near-static dipolar coupling between ^{13}C and ^{1}H spins which is most likely to exist in the more rigid crystalline regions. These in turn would be expected to give the broadest ^{1}H spectrum which, we have shown, is associated with the longer $T_{1\rho}$ components. To illustrate the subtle effects which can arise, we mention the fact that the quenched sample of the α-form shows somewhat different proton $T_{1\rho}$ behaviour and we are presently investigating the quantitative aspects of this problem and its relevance to cross-polarization.

*The α- and β-crystalline forms*

Isotactic polypropylene is known to adopt a helical conformation in the solid with three monomer units per turn (i.e. a 3:1 helix). The various crystalline modifications of polypropylene have been extensively studied[8,9], and *Figure 2* indicates the present view of the arrangement of

the helical molecules in the crystalline region of the α form The view shown is a projection along the helix axis with the corners of the triangles representing the positions of the methyl groups in the 3:1 helix. The circular arrows indicate the handedness of the individual helices. The probability of both left- and right-handed helices being present is real and indeed it is considered that in the α-form the most likely structure contains left and right handed pairs in close proximity as indicated in *Figure 2*. It is considered that these pairs of helices are able to form a closer association because of the ability of left and right handed 'screws' to enmesh. It is evident in this structure that two distinct environments for the monomer unit exist as a result of this interaction between helices of opposite handedness and these are identified in *Figure 2* by the labels A and B. Each corner of the triangles representing the helical polypropylene chains in *Figure 2* can be equated in symmetry terms to the positions of all three carbon atoms of a monomer unit[8] and thus we would expect all three ^{13}C resonance lines to be split into two lines with relative intensities 2:1. As can be seen from *Figure 1a* the spectrum of the annealed sample of the α-isotactic form shows resolved splittings for the methyl and methylene carbons. In addition, careful investigation of the methine carbon resonance indicates the presence of an asymmetric lineshape consistent with the existence of an unresolved splitting of the order of 3 Hz with an intensity distribution in the same sense as those seen for the resonances of the methyl and methylene carbons. Since the form and origin of the lineshapes for the component lines in each spectral region is not known, it is not possible to make an unambiguous deconvolution of the bands to obtain accurate relative areas for the individual lines. However, the appearance of the methylene band, for example, is not inconsistent with a 2:1 intensity distribution, assuming the individual linewidths to be similar. In addition, when the spectra were obtained as a function of contact time, it was found that although the methyl, methine and methylene bands cross-polarized at different rates, as would be expected[10], the intensities within a given band cross-polarized at the same rate. This indicates a similar local environment for the two lines which therefore cannot be assigned individually to amorphous and crystalline components. We therefore assign the lines to the inequivalent sites in the crystal structure, as discussed above. These splittings, all of the order of 1 ppm or less, should be compared with the large splitting of 8.7 ppm we reported for the methylene carbon ^{13}C resonance in syndiotactic polypropylene[1]. In that case the splitting was identified as arising from two inequivalent sites for the methylene carbon intrinsic to the conformation adopted by this form of polypropylene, and its magnitude was explained in terms of a 3-bond intramolecular effect (the γ-effect). The smaller size of the spectral splittings observed for α-isotactic polypropylene is consistent with their being intermolecular in origin as suggested above. *Figure 2* shows that the centre-to-centre distance of the enmeshed pairs of helical chains is 5.28 Å compared with the corresponding smallest distance of 6.15 Å between helices in different pairs. These splittings are thus further examples of crystallographic inequivalences in solid-state n.m.r. spectroscopy[11]. The fact that the methyl and methylene splittings are of similar magnitude whereas that of the methine is an order of magnitude smaller presumably arises from the fact that
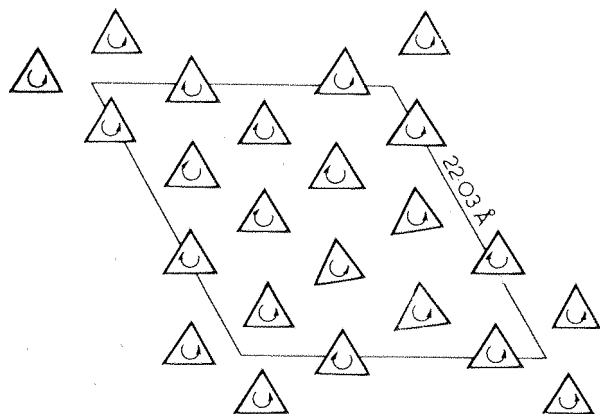
**Figure 3** Structure of the β-form of isotactic polypropylene as proposed from X-ray diffraction[9]. The conventions used are as for **Figure 2**. Note the absence of any pairing of helical chains of opposite handedness and the rotation of the three molecules in the bottom right of the unit cell with respect to the others

this carbon is shielded from intermolecular effects by its methyl substitution. In solution state [13]C n.m.r. it is well known that tacticity effects on the methine resonance of polypropylene are much smaller than those observed for the other carbons[12].

The β form of isotactic polypropylene is also considered to consist of helices with the same 3:1 character as in the α-form. However X-ray diffraction studies indicate that it differs in the way the helices are packed together in the crystalline regions. *Figure 3* illustrates the proposed structure of the β-form as deduced from X-ray studies[9]. As can be seen, the proposed structure indicates the presence of left- and right-handed helices arranged in groups of the same handedness. This arrangement does not allow the close approach of pairs of helices as found in the structure of the α-form. It is to be expected, therefore, that interchain interactions may well be less in the β form, and this probably accounts for the absence of any resolvable splittings in the spectrum of this form. The structure shown in *Figure 3* implies the existence of inequivalent sites but, because of the relatively large centre-to-centre separation of the helices in this structure, any splittings arising from such effects would be expected to be small. It is perhaps significant however that the methyl carbon resonance is broader than the methylene or methine resonances in the spectrum of the β form, which would be expected if a number of unresolved splittings existed since the methyl groups, being on the outside of the helices, would be the most affected by neighbouring chains which are not capable of enmeshing as in the α form.

### Quenched α form

The spectrum of this sample differed considerably from that of the annealed sample. The main changes observed were (i) a shift in the frequencies of the maximum peak intensities in the methyl and methylene regions to coincide with those of the lower intensity lines in these regions for the annealed sample and (ii) an apparent lowering of resolution in that the splittings, whilst still discernible, only appear as shoulders. As noted above, the proton $T_{1\rho}$ behaviour shows some differences from that of the annealed sample. The relaxation is still three-component but the proportions and particularly the

relaxation times of the components are different. Simple quantitative considerations show that it is not possible to explain the changes in the ^{13}C spectra by assuming that somehow the spectrum of the amorphous region has now been added by comparison with that of the annealed sample. On this basis it is clear that there has been a transfer of resonance intensity to the chemical shift characteristic of the outer, less perturbed, methyl/methylene environments of *Figure 2*. X-ray diffraction data on quenched polypropylene show broader reflections and intensity changes in comparison with annealed samples but confirm that it is still basically in the α-form. The usual interpretation of these X-ray observations is to suggest a wider range of positions for the helical molecules in the unit cell and/or that the crystal size and perfection is much reduced. Since the n.m.r. data indicate that the environment of the methyl and methylene groups is less distinct, indeed that the resonance frequency favoured is that assigned to the outer position in the 'enmeshed' pair of helices, it is considered that these pairs of helices are more separated in the quenched state to give a more open structure. Whether this may be thought of in terms of trapped defects in the structure, e.g. helices which are translated with respect to each other or similar effects, is not easily decided.

### Chemical shift differences

In addition to the obvious differences between the α and β forms of polypropylene referred to, close examination of the comparative chemical shift values reveals interesting differences. Again, because of the external referencing procedures one must exercise caution in making comparisons but there are clearly significant relative differences as the figures in *Table 1* show. For example, the methyl resonance in the β form is close to or slightly to high frequency of the methyl line of relative intensity 2 in the α-form whilst the methylene resonance falls between the two in the α-form. These small differences could arise from a number of effects. Firstly, the exact distances between the chains are different in the two structures, which could lead to small shift differences. Secondly, it is possible that the proximity of the internal methyl groups in the enmeshed pairs causes distortion which could also lead to small chemical shift differences. Calculations performed on the measured X-ray data for the α form[13] show that there are probably two minor changes in the positioning of the internal methyl groups due to the way in which helices traverse the unit cell as discussed by Wunderlich[14]. In principle then, it is possible that there is a further, unresolved splitting on the higher intensity methyl resonance of the α-form.

## CONCLUSIONS

The information obtained from the ^{13}C high-resolution spectrum of solid isotactic polypropylene demonstrates the potential of this method for the investigation of the details of molecular structure in the solid state. Not only may intramolecular effects be seen in terms of chemical shifts but intermolecular effects also clearly give rise to subtle changes in both signal intensities and chemical shifts. Thus, it has been demonstrated that different morphologies give rise to recognizably different spectra, enabling the n.m.r. technique to distinguish between the α and β crystalline forms of isotactic polypropylene.

Changes in the packing of molecules, which arise when less perfect crystals are formed, for example in quenched samples, can be detected, and the concept of more open helical pairs in the quenched form has been proposed to explain these changes whilst the unit cell configuration is still retained.

## ACKNOWLEDGEMENTS

## REFERENCES

1   Bunn, A., Cudby, M. E. A., Harris, R. K., Packer, K. J. and Say, B. J. *J. Chem. Soc. Chem. Comm.* 1981, 15
2   Pines, A., Gibby, M. G. and Waugh, J. S. *J. Chem. Phys.* 1973, **59**, 569
3   Balimann, G., Burgess, M. J. S., Harris, R. K., Oliver, A. G., Packer, K. J., Say, B. J., Tanner, S. F., Blackwell, R. W., Brown, L. W., Bunn, A., Cudby, M. E. A. and Eldridge, J. W. *Chem. Phys.* 1980, **46**, 469
4   Anderson, W. A. *Rev. Sci. Instrum.* 1961, **32**, 241
5   Solomon, I. *C.R. Acad. Sci. Paris* 1959, **248**, 92
6   Heatley, F., Salovey, R. and Bovey, F. A. *Macromolecules* 1969, **2**, 619
7   McBrierty, V. J. *Faraday Discuss. Chem. Soc.* 1979, **68**, 78
8   Natta, G. and Corradini, P. *Nuovo Cimento* 1960, **15**, 1, 40
9   Turner-Jones, A., Aizlewood, Jean M. and Beckett, D. R. *Makromol. Chem.* 1964, **75**, 134
10  Demco, D. E., Tegenfeldt, J. and Waugh, J. S. *Phys. Rev.* 1975, **B11**, 4133
11  Balimann, G. E., Groombridge, C. J., Harris, R. K., Packer, K. J., Say, B. J. and Tanner, S. F. *Phil. Trans. R. Soc. Lond.* 1981, **A299**, 643
12  Randall, J. C. 'Polymer sequence determination, Carbon-13 NMR method', Academic Press, 1977, p. 21
13  Blundell, D. J. private communication
14  Wunderlich, B. 'Macromolecular Physics', Vol. 1, Academic Press, 1973, p. 78